

# Desensitization and binding properties determine distinct $\alpha 1\beta 2\gamma 2$ and $\alpha 3\beta 2\gamma 2$ GABA<sub>A</sub> receptor-channel kinetic behavior

Andrea Barberis,<sup>1</sup> Jerzy W. Mozrzymas,<sup>1,3</sup> Pavel I. Ortinski<sup>1,2</sup> and Stefano Vicini<sup>1,2</sup>

<sup>1</sup>Department of Physiology and Biophysics and

<sup>2</sup>Interdisciplinary Program in Neuroscience, Georgetown University School of Medicine, 225 Basic Research Building, 3900 Reservoir Road, NW Washington, DC 20007, USA

<sup>3</sup>Laboratory of Neuroscience, Department of Biophysics, Wrocław Medical University, Wrocław, Poland

**Keywords:** GABA, kinetics, patch clamp, rat, subunit

## Abstract

GABA<sub>A</sub> receptor subtypes comprising the  $\alpha 1$  and  $\alpha 3$  subunits change with development and have a specific anatomical localization in the adult brain. These receptor subtypes have been previously demonstrated to greatly differ in deactivation kinetics but the underlying gating mechanisms have not been fully elucidated. Therefore, we expressed rat  $\alpha 1\beta 2\gamma 2$  and  $\alpha 3\beta 2\gamma 2$  receptors in human embryonic kidney 293 cells and recorded current responses to ultrafast GABA applications at macroscopic and single-channel levels. We found that the slow deactivation of  $\alpha 3\beta 2\gamma 2$ -mediated currents is associated with a relatively small rate and extent of apparent desensitization. In contrast, responses mediated by  $\alpha 1\beta 2\gamma 2$  receptors had faster deactivation and stronger desensitization.  $\alpha 3\beta 2\gamma 2$  receptors had faster recovery in the paired-pulse agonist applications than  $\alpha 1\beta 2\gamma 2$  channels. The onset of currents mediated by  $\alpha 3\beta 2\gamma 2$  receptors was slower than that of  $\alpha 1\beta 2\gamma 2$  for a wide range of GABA concentrations. Single-channel analysis did not reveal differences in the opening/closing kinetics of  $\alpha 1\beta 2\gamma 2$  and  $\alpha 3\beta 2\gamma 2$  channels but burst durations were longer in  $\alpha 3\beta 2\gamma 2$  receptors. Simulation with a previously reported kinetic model was used to explore the differences in respective rate constants. Reproduction of major kinetic differences required a smaller desensitization rate as well as smaller binding and unbinding rates in  $\alpha 3\beta 2\gamma 2$  compared with  $\alpha 1\beta 2\gamma 2$  receptors. Our work describes the mechanisms underlying the kinetic differences between two major GABA<sub>A</sub> receptor subtypes and provides a framework to interpret data from native GABA receptors.

## Introduction

GABA<sub>A</sub> receptors (GABA<sub>A</sub>Rs) are pentameric structures and as many as 20 subunits ( $\alpha 1$ – $6$ ,  $\beta 1$ – $4$ ,  $\gamma 1$ – $3$ ,  $\delta$ ,  $\rho 1$ – $3$ ,  $\epsilon$ ,  $\pi$  and  $\theta$ ) have been cloned so far (Fritschy & Brunig, 2003). The kinetics and pharmacology of GABA<sub>A</sub>Rs strictly depend on their subunit composition (Whiting, 2003).  $\alpha$  subunits are critical determinants of ligand binding and of activation, deactivation and desensitization kinetics of GABA-induced responses of native and recombinant GABA<sub>A</sub>Rs (Verdoorn, 1994; Gingrich *et al.*, 1995; Lavoie *et al.*, 1997; McClellan & Twyman, 1999; Bohme *et al.*, 2004). Such  $\alpha$  subunit dependence of GABA<sub>A</sub>R function appears to be associated with differential localization and the specific functions of these receptors in the central nervous system (Pirker *et al.*, 2000; for review see Rudolph & Mohler, 2004). Receptors containing the  $\alpha 3$  subunit are characterized by slow deactivation, slow desensitization onset and low affinity (Verdoorn, 1994; Gingrich *et al.*, 1995). Such a peculiar kinetic pattern has been shown to play an important role in the regulation of the network temporal resolution in the early development stage (Ortinski *et al.*, 2004).  $\alpha 3$ -containing receptors have been shown to be abundant in serotonergic neurons in Raphe nuclei (Gao *et al.*,

1993) and Browne *et al.* (2001) attributed the slow GABAergic current kinetics observed in thalamic neurons to the presence of the  $\alpha 3$  subunit. Although the physiological relevance of the spatial and temporal differential expression of  $\alpha 3$ -containing receptors in the brain is still unclear, it is likely that the  $\alpha 3$  subunit could efficiently serve as a prolonged and sustained synaptic GABAergic control. Thus, it is convenient to investigate the kinetic features of  $\alpha 3\beta 2\gamma 2$  receptors in comparison to the  $\alpha 1\beta 2\gamma 2$  receptor subtype that has been extensively studied and is believed to be most abundantly expressed among all GABA<sub>A</sub>Rs in the central nervous system (Whiting, 2003). Verdoorn (1994) and Gingrich *et al.* (1995) have analysed the currents elicited by exogenous GABA applications and found profound differences in activation, deactivation and desensitization kinetics between currents mediated by  $\alpha 1$  and  $\alpha 3$  subunit-containing receptors. Although Verdoorn (1994) did not address a detailed determination of receptor gating, Gingrich *et al.* (1995) adapted the model of Twyman *et al.* (1990) and concluded that the differences between binding and unbinding rates were nearly sufficient to account for the functional differences between  $\alpha 1\beta 2\gamma 2$  and  $\alpha 3\beta 2\gamma 2$  receptors observed in their experiments. However, a limited temporal resolution of these recordings (application time <30 ms, Gingrich *et al.*, 1995) might have precluded detection of the fastest current components. For instance, in some neuronal and recombinant GABA<sub>A</sub>Rs, the onset of rapid desensitization occurs within a millisecond time scale (Jones &

Correspondence: Dr Stefano Vicini, <sup>1</sup>Department of Physiology and Biophysics, as above.  
E-mail: svicini01@georgetown.edu

Received 1 September 2006, revised 1 March 2007, accepted 9 March 2007

Westbrook, 1995; McClellan & Twyman, 1999; Mozrzymas *et al.*, 2003a,b). Furthermore, rapid desensitization has been demonstrated to play a pivotal role in shaping deactivation and synaptic decay of GABAergic currents (Jones & Westbrook, 1995). Thus, we further explored the gating mechanisms of  $\alpha 3$  subunit-containing GABA<sub>A</sub>Rs at high temporal resolution and thoroughly addressed the role of the desensitization process in shaping deactivation kinetics (Jones & Westbrook, 1995). We used ultrafast GABA applications to elicit macroscopic and single-channel currents mediated by recombinant  $\alpha 1\beta 2\gamma 2$  and  $\alpha 3\beta 2\gamma 2$  receptors, expressed in human embryonic kidney 293 cells. The study of such currents revealed that these two receptor subtypes differ in both affinity and gating properties. We conclude therefore that, with respect to  $\alpha 1\beta 2\gamma 2$ ,  $\alpha 3\beta 2\gamma 2$  receptors are characterized by both a slower binding/unbinding rate constant and a slower desensitization onset.

Based on our model simulations, as a matter of speculation, we also propose that both receptor types might experience transitions between singly- and doubly-bound desensitized states.

## Materials and methods

### Human embryonic kidney 293 cell line

Human embryonic kidney 293 cells (no. CRL1573, American Type Culture Collection, Rockville, MD, USA) were grown in minimal essential medium (Invitrogen Corporation, Carlsbad, CA, USA), supplemented with 10% fetal bovine serum, 100 units/mL penicillin and 100 units/mL streptomycin (Invitrogen Corporation), in a 5% CO<sub>2</sub> incubator. Exponentially growing cells were dispersed with trypsin, seeded at  $2 \times 10^5$  cells/35 mm dish in 1.5 mL of culture medium and plated on 12 mm glass coverslips (Fisher Scientific, Pittsburgh, PA, USA).

### cDNA transient transfection

Rat  $\alpha 1$ ,  $\beta 2$  and  $\gamma 2_s$  GABA<sub>A</sub>R subunit cDNAs were individually subcloned into the expression vector pGW1 and were kindly provided by Dr Trevor Smart (University College London, UK). Rat  $\alpha 3$  subunit was subcloned into the expression vector pRK5 and was a gift of Dr Hartmut Lüddens (University of Mainz, Germany). Human embryonic kidney 293 cells were transfected using the calcium phosphate precipitation method (Chen & Okayama, 1987). The following plasmid combinations were mixed:  $\alpha 1:\beta 2:\gamma 2$  and  $\alpha 3:\beta 2:\gamma 2$  (1  $\mu$ g for  $\alpha$  and  $\beta$  cDNAs, respectively, and 3  $\mu$ g for  $\gamma$  cDNA) and the coprecipitates were added to culture dishes containing 1.5 mL minimal essential medium for 12–16 h at 37 °C under 3% CO<sub>2</sub>. The medium was removed, and the cells were rinsed twice with culture medium and finally incubated in the same medium for 24 h at 37 °C under 5% CO<sub>2</sub>. Cotransfection with the plasmid pEGFP (Invitrogen Corporation) allowed easy recognition of transfected cells expressing this fluorescent marker. More than 90% of the cells expressing enhanced green fluorescent protein also expressed GABA<sub>A</sub>Rs.

### Electrophysiological recordings

At a GABA concentration of at least 100  $\mu$ M, current responses were recorded in the outside-out configuration of the patch-clamp technique using the Axopatch 200B amplifier (Molecular Device Corporation, Sunnyvale, CA, USA). However, in the excised patch mode, currents elicited by 30  $\mu$ M GABA (or lower) were often too small to reliably quantify their time course (especially onset kinetics) and, for this

GABA concentration range, recordings were preferentially made in the whole-cell configuration selecting cells with small diameter and capacitance of less than 8 pF (small lifted cells). Kinetics of current responses recorded from excised patches and from lifted cells did not show any clear difference and were pooled together. In all experiments, the pipette voltage was set at  $-70$  mV. Patch electrodes, formed from thin borosilicate glass (Wiretrol II, Drummond Scientific, Broomall, PA, USA), had a resistance of 6–8 M $\Omega$  when filled with an intracellular solution containing (in mM): CsCl, 145; CaCl<sub>2</sub>, 1; 1,2-bis(2- amino-phenoxy)ethane-N,N,N',N'-tetra-acetic acid, 11; MgATP, 4; HEPES, 10 (pH 7.2 with CsOH). The composition of the external solution was (in mM): NaCl, 145; KCl, 5; CaCl<sub>2</sub>, 1; MgCl<sub>2</sub>, 1; glucose, 5; HEPES, 5 (pH 7.4 with NaOH). All experiments were performed at room temperature (22–24 °C). Single-channel currents were recorded in the outside-out configuration of the patch-clamp technique. Patches with a low number of channels (apparently one to three channels) were used for single-channel recordings. The occurrence of such patches was rare, only one out of 10–20. For the analysis requiring a high temporal resolution (e.g. rise time kinetics of evoked currents), the signals were low-pass filtered at 10 kHz with an eight-pole Bessel filter, sampled at 50–125 kHz using the analog-to-digital converter Digidata 1322A (Molecular Device Corporation) and stored on the computer hard disk. PCLAMP 9.2 (Molecular Device Corporation) software was used for acquisition and data analysis. The single-channel currents were acquired at 50 kHz. Single-channel current records in figures were filtered at 0.9 kHz for display purposes.

### Drug application

GABA-containing solution was applied to excised patches using an ultrafast perfusion system based on a piezoelectric-driven theta-glass application pipette (Jonas, 1995). The piezoelectric translator used was the P-245.30 Stacked Translator (Physik Instrumente, Waldbronn, Germany) and theta glass tubing was from Hilgenberg (Malsfeld, Germany). The open tip recordings of the liquid junction potentials revealed that the 10–90% exchange of solution occurred within 60–100  $\mu$ s. The speed of the solution exchange was also estimated around the excised patch by the 10–90% onset of the membrane depolarization induced by application of high (25 mM) potassium saline. In this case, the 10–90% rise time value (70–120  $\mu$ s) was very close to that found for the open tip recordings. Amplitude and deactivation kinetics were within 5% of the initial values in most experiments. Recordings with greater changes were discarded.

### Analysis

The decaying phase of the currents was fitted with a function in the form:

$$y(t) = \sum_{i=1}^n A_i \exp(-t/\tau_i) \quad (1)$$

where  $A_i$  are the fractions of respective components ( $\sum A_i = 1$ ) and  $\tau_i$  are the time constants. The deactivation time course was well fitted with a sum of three exponentials ( $n = 3$ ). The averaged deactivation time constant  $\tau_w$  was calculated using the formula  $\tau_w = \sum A_i \tau_i$ . The time course of desensitization onset was described using Eq. 1 (sum of exponential functions) with a constant value representing the steady-state current during a continuous application of saturating [GABA].

A standard paired-pulse protocol (pulse duration 2 ms and saturating [GABA]) was used to study the recovery process. The extent of

recovery was expressed in terms of the recovery parameter ( $R$ ) given by the following formula:

$$R = \frac{I_2 - I_3}{I_1 - I_3} \quad (2)$$

where  $I_1$  is the first peak amplitude,  $I_2$  is the second peak amplitude and  $I_3$  is the current value immediately before the application of the second pulse.

The rate of onset was calculated as a reciprocal of the time constant of exponential function fitted to the current rising phase. The relationship between the time constant describing the current onset and the 10–90% rise time is:

$$10\text{--}90\% \text{ rise time} = \ln(9) \cdot \tau$$

The kinetic modeling was performed with the Channel Lab 2.0 software (developed by S. Traynelis for Synaptosoft, Decatur, GA, USA), which converted the kinetic model (Fig. 8) into a set of differential equations and solved them numerically assuming, as the initial condition, that at  $t = 0$  no bound or open receptors were present.

For each protocol used, we compared point-by-point the normalized individual simulated traces with the normalized and averaged experimentally recorded traces. The goodness of fit was estimated by calculating the normalized residuals (sum of squares differences divided by the number of samples) according to the formula

$$res = \frac{\sum_{i=1}^n (y_i^{\text{mod}} - y_i^{\text{exp}})^2}{n} \quad (3)$$

where  $y^{\text{mod}}$  and  $y^{\text{exp}}$  are the modelled and experimentally measured values, respectively, and  $n$  is the number of samples in the traces (Traynelis, Channel Lab). Using such a procedure, we compared the experimental traces with the outputs of the frame model of Jones & Westbrook (1995); the overall normalized residuals values obtained for the tested protocols were  $2.2 \times 10^{-3}$  and  $9.7 \times 10^{-3}$  for  $\alpha 1\beta 2\gamma 2$  and  $\alpha 3\beta 2\gamma 2$  receptors. By using the frame model of Jones *et al.* (1998) the normalized residuals were  $1.9 \times 10^{-3}$  and  $2.7 \times 10^{-3}$  for  $\alpha 1\beta 2\gamma 2$  and  $\alpha 3\beta 2\gamma 2$  receptors, respectively. These values indicate that the frame model of Jones *et al.* (1998) provided a better reproduction of our experimental data.

### Single-channel analysis

For off-line analysis of single-channel events, current traces were low-pass filtered at 2 kHz with the digital Bessel filter at  $-3$  dB cutoff frequency of PCLAMP 9.2 software. Open and closed events were distinguished by applying the 50% criterion. Occasionally, openings at lower conductance or substates were observed but their frequency was less than 1% and they were discarded. The overlapping events present in the considered records were excluded from the analysis. Dead time used to define the minimal detectable event duration with our filter setting was 0.09 ms (Colquhoun & Sigworth, 1995). To define the end-burst critical closed times, the closed time distributions were constructed and fitted with four or five exponential components (confidence interval 95%). For each receptor subtype, in all considered distributions, the two shortest components ( $\sim 0.4$  and 1.9 ms) were almost always much shorter with respect to the slower components. Moreover, the slower time constants showed substantial variability

depending on the number of channels in the patch. Thus, the two shortest components were interpreted as intraburst closures and the critical time ( $T_{\text{crit}}$ ) was calculated by equalizing the proportion of misclassifications using the following formula (Colquhoun & Sakmann, 1985):

$$1 - \exp(-T_{\text{crit}}/\tau_{\text{burst}}) = \exp(-T_{\text{crit}}/\tau_{\text{extraburst}}) \quad (4)$$

All experiments were performed at room temperature (22–24 °C). Data are expressed as mean  $\pm$  SEM and unpaired Student's  $t$ -tests were used for data comparison.

## Results

### Slower GABA binding rate for $\alpha 3\beta 2\gamma 2$ compared with $\alpha 1\beta 2\gamma 2$ receptor

The activation of GABA<sub>A</sub>R (as of any other ligand-gated channel) consists of at least two kinetically distinct steps including binding of the agonist to the receptor and the conformational transitions of bound receptor. Although the binding rate is assumed to be proportional to the agonist concentration, the rates of the conformational changes are concentration independent. Thus, at sufficiently low agonist concentration, the receptor activation would critically depend on the binding rate and therefore the current onset kinetics is expected to show a strong agonist concentration dependence. To assess differences in the binding rate, current responses to non-saturating [GABA] in the range 10–300  $\mu\text{M}$  were recorded for  $\alpha 1\beta 2\gamma 2$  or  $\alpha 3\beta 2\gamma 2$  receptors. As shown in Fig. 1, at each GABA concentration used, currents mediated by  $\alpha 3\beta 2\gamma 2$  receptors were characterized by onset rates slower by more than one order of magnitude than those of  $\alpha 1\beta 2\gamma 2$  receptors. These data provide strong evidence that the binding rate of  $\alpha 3\beta 2\gamma 2$  receptors is much slower than that of  $\alpha 1\beta 2\gamma 2$  channels. However, it needs to be considered that, even at non-saturating [GABA], the time course of the current onset phase is not shaped exclusively by the binding rate. For instance, as previously pointed out by Mozrzymas *et al.* (2003a), the rising phase of currents elicited by a wide range of GABA concentrations may be affected by rapid desensitization as well as by opening/closing transitions between bound states. Moreover, at low [GABA], current onset is additionally shaped by the unbinding rate (Maconochie *et al.*, 1994). Thus, precise comparison of binding properties of these two receptor types requires additional information on kinetic properties of these channels.

### Onsets of saturated responses are slower for $\alpha 3\beta 2\gamma 2$ than for $\alpha 1\beta 2\gamma 2$ channels

Although at non-saturating [GABA] the onset of current responses is strongly dependent on agonist concentration, when applying saturating [GABA] the binding step occurs very quickly and the current onset reflects the kinetics of conformational transitions between bound states. We first analysed the 10–90% rise time of current evoked pulses of 10 mM GABA, a concentration known to saturate the onset kinetics of  $\alpha 1\beta 2\gamma 2$ -mediated currents. We found that the  $\alpha 3\beta 2\gamma 2$ -mediated currents showed a rise time significantly slower than that in  $\alpha 1\beta 2\gamma 2$ -mediated currents ( $0.29 \pm 0.02$  and  $1.01 \pm 0.08$  ms, respectively,  $P < 0.05$ , Fig. 2A and B). However, as reported above, the  $\alpha 3\beta 2\gamma 2$  receptor binding rate constant ( $k_{\text{on}}$ ) is much slower than in  $\alpha 1\beta 2\gamma 2$  channels. Thus, 10 mM GABA might be insufficient to saturate the rising phase of responses mediated by  $\alpha 3\beta 2\gamma 2$  receptors. In order to test this possibility, the GABA concentration was increased up to 30,

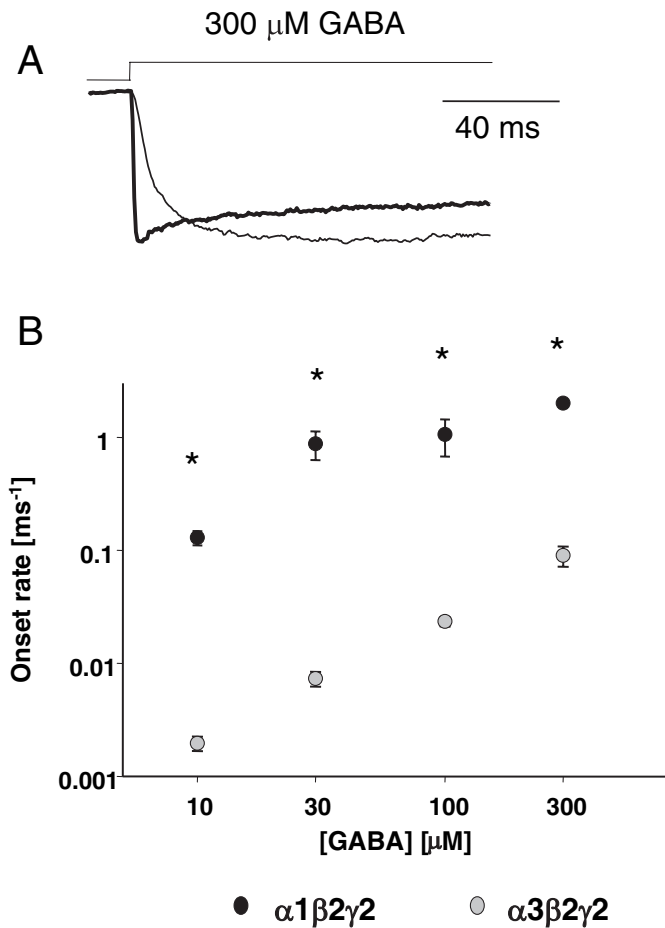


FIG. 1. Comparison of rise time for currents elicited by non-saturating GABA in  $\alpha 1\beta 2\gamma 2$  and  $\alpha 3\beta 2\gamma 2$  channels. (A) Typical examples of normalized  $\alpha 1\beta 2\gamma 2$ - and  $\alpha 3\beta 2\gamma 2$ -mediated current responses to a non-saturating (300  $\mu\text{M}$ ) GABA concentration. (B) Summary of data derived for the assessment of the onset rate of current elicited at four increasing non-saturating GABA concentrations in at least five patches excised from human embryonic kidney cells expressing  $\alpha 1\beta 2\gamma 2$  and  $\alpha 3\beta 2\gamma 2$  receptors. \* $P < 0.05$  indicates a significant difference. Note that the difference in the onset rate is so large between the two combinations that the vertical axis is shown in logarithmic scale.

50 and 60 mM. As expected, the rise time of the  $\alpha 1\beta 2\gamma 2$ -mediated current evoked by 30 mM GABA was not significantly different from that elicited by 10 mM GABA ( $0.27 \pm 0.02$  ms,  $n = 4$  and  $0.29 \pm 0.02$  ms,  $n = 4$ , respectively, Fig. 2A and B), confirming that 10 mM GABA is saturating for these receptors. In contrast, the 10–90% rise times of  $\alpha 3\beta 2\gamma 2$ -mediated currents obtained at 30 and 50 mM GABA were significantly accelerated with respect to that at 10 mM GABA ( $0.59 \pm 0.05$  ms,  $n = 6$ ,  $P < 0.05$  and  $0.41 \pm 0.01$  ms,  $n = 4$ ,  $P < 0.05$ , Fig. 2A and B). The decrease in the 10–90% rise time was significant between applications of 30 and 50 mM GABA ( $P < 0.05$ ). A further increase of [GABA] from 50 to 60 mM did not significantly accelerate the current onset kinetics ( $0.42 \pm 0.04$  ms,  $n = 6$ ), indicating that saturation of the activation process was reached. Altogether, the rising phase of currents elicited by saturating [GABA] is significantly slower for responses mediated by  $\alpha 3\beta 2\gamma 2$  than  $\alpha 1\beta 2\gamma 2$  receptors, indicating that the conformational changes underlying the onset of  $\alpha 3\beta 2\gamma 2$ -mediated currents are slower than those in  $\alpha 1\beta 2\gamma 2$  receptors. This finding might suggest that  $\alpha 3\beta 2\gamma 2$  channels are endowed with a slower opening/closing kinetics of fully-bound receptors. However, the onset of currents evoked by saturating

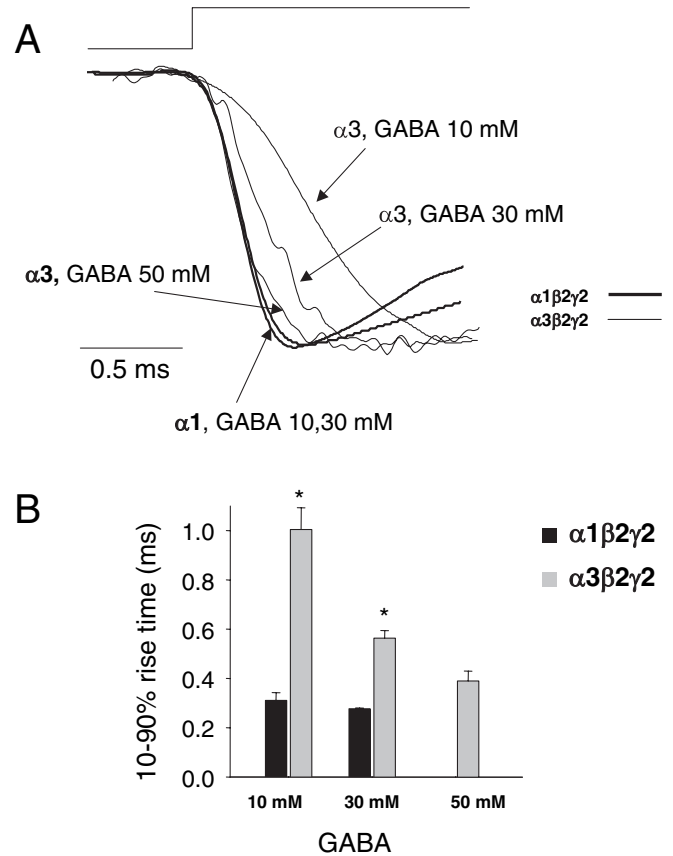


FIG. 2. Comparison of rise time currents elicited by high GABA concentration between  $\alpha 1\beta 2\gamma 2$  and  $\alpha 3\beta 2\gamma 2$  channels. (A) Typical examples of normalized  $\alpha 1\beta 2\gamma 2$ - and  $\alpha 3\beta 2\gamma 2$ -mediated current responses to high GABA concentrations. Arrows point to responses to a distinct concentration for distinct subunit combinations. Note that whereas for  $\alpha 1\beta 2\gamma 2$  10 mM GABA saturates the onset rate, in  $\alpha 3\beta 2\gamma 2$ -mediated responses onset saturation is achieved at 50 mM GABA. (B) Summary of data deriving for the assessment of the 10–90% rise time of current elicited at three distinct concentrations as indicated in at least four patches excised from human embryonic kidney cells expressing  $\alpha 1\beta 2\gamma 2$  and  $\alpha 3\beta 2\gamma 2$  receptors. \* $P < 0.05$  indicates a significant difference between subunits.

[GABA] may depend additionally on desensitization kinetics (Mozrzymas *et al.*, 2003a).

It should additionally be noted that, although for  $\alpha 1\beta 2\gamma 2$  and  $\alpha 3\beta 2\gamma 2$  receptors a saturation of the onset kinetics is reached at  $\sim 10$  and 50 mM, respectively, saturation of the peak amplitude is achieved at agonist concentration one order of magnitude lower. Thus, 10 mM GABA represents a dose able to saturate the peak of currents mediated by both  $\alpha 1\beta 2\gamma 2$  and  $\alpha 3\beta 2\gamma 2$  receptors. Moreover, no differences in deactivation of currents mediated by  $\alpha 3\beta 2\gamma 2$  receptors were observed when applying 10, 30 or 50 mM GABA (not shown).

#### $\alpha 3\beta 2\gamma 2$ -mediated currents show slower deactivation kinetics with respect to $\alpha 1\beta 2\gamma 2$ -mediated currents

To compare the deactivation kinetics of  $\alpha 1\beta 2\gamma 2$  and  $\alpha 3\beta 2\gamma 2$  receptors, current responses elicited by brief (2 ms) pulses of saturating GABA concentration were analysed (Fig. 3A, for reasons explained above, 10 mM was used for  $\alpha 1\beta 2\gamma 2$  and 50 mM for  $\alpha 3\beta 2\gamma 2$ ). The decaying phase of currents mediated by  $\alpha 1\beta 2\gamma 2$  or  $\alpha 3\beta 2\gamma 2$  channels was best fitted with a triple exponential function. Currents mediated by  $\alpha 3\beta 2\gamma 2$

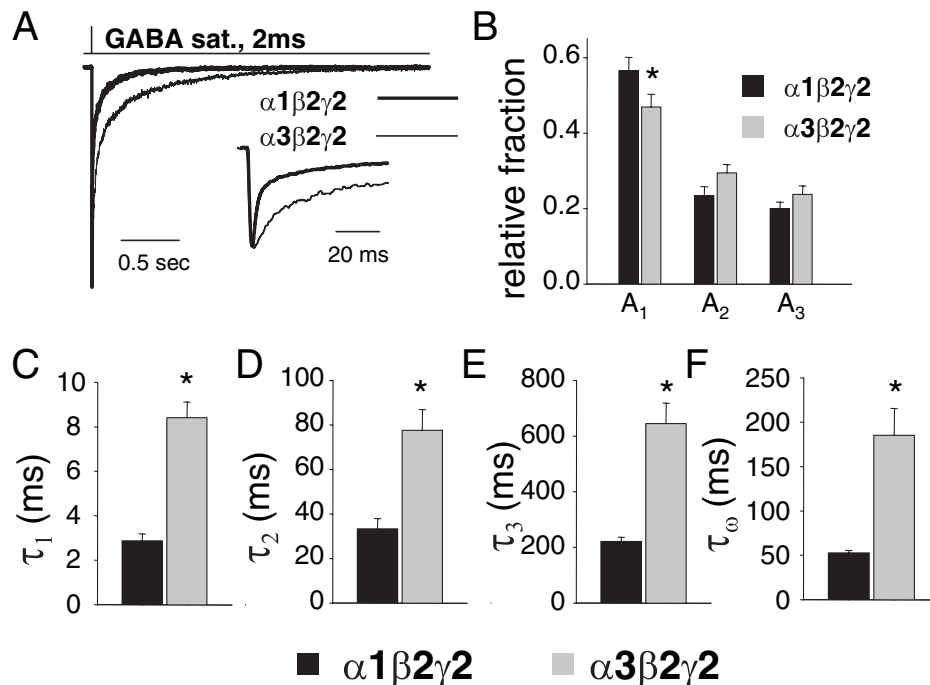


FIG. 3. Comparison of deactivation kinetics for currents elicited by brief GABA pulses between  $\alpha 1\beta 2\gamma 2$  and  $\alpha 3\beta 2\gamma 2$  channels. (A) Normalized average of 10 responses induced by 2 ms applications of saturating GABA (GABA sat.) to a patch excised from human embryonic kidney cells expressing  $\alpha 1\beta 2\gamma 2$  (10 mM GABA) and  $\alpha 3\beta 2\gamma 2$  (50 mM GABA) receptors. Average currents are shown superimposed with a thick line for  $\alpha 1\beta 2\gamma 2$  receptors and a thin line for  $\alpha 3\beta 2\gamma 2$  receptors. Inset: the same currents at an expanded time scale. (B–E) Summary of the parameters derived from a triple exponential fitting of decay of  $\alpha 1\beta 2\gamma 2$  and  $\alpha 3\beta 2\gamma 2$  receptor GABA-gated currents with (in B) the relative contribution of each component to peak amplitude ( $A_1$ – $A_3$ ) and (in C–E) each of the time constants. (F) Weighted averages of deactivation time constants are shown for  $\alpha 1\beta 2\gamma 2$ - and  $\alpha 3\beta 2\gamma 2$ -mediated currents. Each bar represents the mean  $\pm$  SEM of six patches for  $\alpha 1\beta 2\gamma 2$  receptors and nine patches for  $\alpha 3\beta 2\gamma 2$  receptors studied. Traces are normalized to the same peak amplitude. \* $P < 0.05$  indicates a significant difference between subunits.

receptors showed a markedly slower decay kinetics than in the case of the  $\alpha 1\beta 2\gamma 2$  channels, with decay weighted time constants ( $\tau_w$ ) of  $185.3 \pm 30.1$  and  $52.5 \pm 2.9$  ms, respectively ( $P < 0.05$ , Fig. 3F). The fast ( $\tau_1$ ), middle ( $\tau_2$ ) and slow ( $\tau_3$ ) time constants obtained for  $\alpha 1\beta 2\gamma 2$  currents were  $2.8 \pm 0.3$ ,  $33.4 \pm 4.6$  and  $221.35 \pm 14.9$  ms ( $n = 6$ ), respectively (Fig. 3C–E), and the weight of the fast component ( $A_1$ ) was predominant with respect to the middle ( $A_2$ ) and the slow ( $A_3$ ), being  $0.57 \pm 0.04$ ,  $0.23 \pm 0.02$  and  $0.20 \pm 0.03$ , respectively (Fig. 3B). The decay time constants for currents mediated by  $\alpha 3\beta 2\gamma 2$  channels were roughly three times slower than those determined for  $\alpha 1\beta 2\gamma 2$  receptor-mediated responses ( $8.4 \pm 0.7$ ,  $77.5 \pm 9.3$  and  $645.1 \pm 73.6$  ms,  $n = 9$ , for  $\tau_1$ ,  $\tau_2$  and  $\tau_3$ , respectively, Fig. 3C–E,  $P < 0.05$  for comparison of each respective time constant). Moreover, similarly to that observed for  $\alpha 1\beta 2\gamma 2$  receptors (although to a lesser extent), the weight of the fast component ( $A_1$ ) in responses mediated by  $\alpha 3\beta 2\gamma 2$  channels was predominant with respect to  $A_2$  and  $A_3$  ( $0.47 \pm 0.03$ ,  $0.29 \pm 0.02$  and  $0.24 \pm 0.02$ , respectively,  $n = 9$ , Fig. 3B). However, the relative weight of the fast component observed for  $\alpha 1\beta 2\gamma 2$  ( $0.57 \pm 0.04$ ,  $n = 6$ ) was significantly larger than that in  $\alpha 3\beta 2\gamma 2$  receptor-mediated currents ( $0.47 \pm 0.03$ ,  $n = 9$ ,  $P < 0.05$ , Fig. 3B).

The pronounced differences in decay kinetics determined for  $\alpha 1\beta 2\gamma 2$  and  $\alpha 3\beta 2\gamma 2$  receptors indicate profound differences in the gating properties of these two receptor subtypes. As a saturating GABA concentration was used, the time evolution of currents is expected to depend mainly on the kinetics of conformational transitions between bound states and on the unbinding rate. In

particular, such a substantial difference in the slow deactivation components (Fig. 3) potentially represents differences in the opening/closing, desensitization/resensitization and unbinding rates. However, the analysis of the deactivation kinetics alone cannot provide sufficient information to reliably estimate so many distinct rate constants and therefore additional results from different experimental protocols were needed.

#### *Faster rate and larger extent of apparent desensitization for $\alpha 1\beta 2\gamma 2$ compared with $\alpha 3\beta 2\gamma 2$ receptors*

The deactivation time course has been shown to critically depend on the desensitization kinetics (Jones & Westbrook, 1995). Moreover, as already mentioned above, different onset rates of currents elicited by saturating [GABA] for  $\alpha 1\beta 2\gamma 2$  and  $\alpha 3\beta 2\gamma 2$  receptors (Fig. 2) might involve differences in the desensitization process in the two receptors. Thus, in order to explore the gating properties of these two receptors it is crucial to describe their desensitization kinetics. For this purpose, currents evoked by prolonged applications of saturating [GABA] were studied. Figure 4A shows examples of currents evoked by long pulses (3 s) of saturating [GABA]. Currents mediated by  $\alpha 1\beta 2\gamma 2$  and  $\alpha 3\beta 2\gamma 2$  channels (in the 3 s time window considered) showed a sharp peak followed by fading, characterized by at least three exponential components. However, the apparent desensitization time courses observed in  $\alpha 1\beta 2\gamma 2$  and  $\alpha 3\beta 2\gamma 2$  receptor-mediated currents were remarkably different. In particular,  $\alpha 1\beta 2\gamma 2$ -mediated currents showed

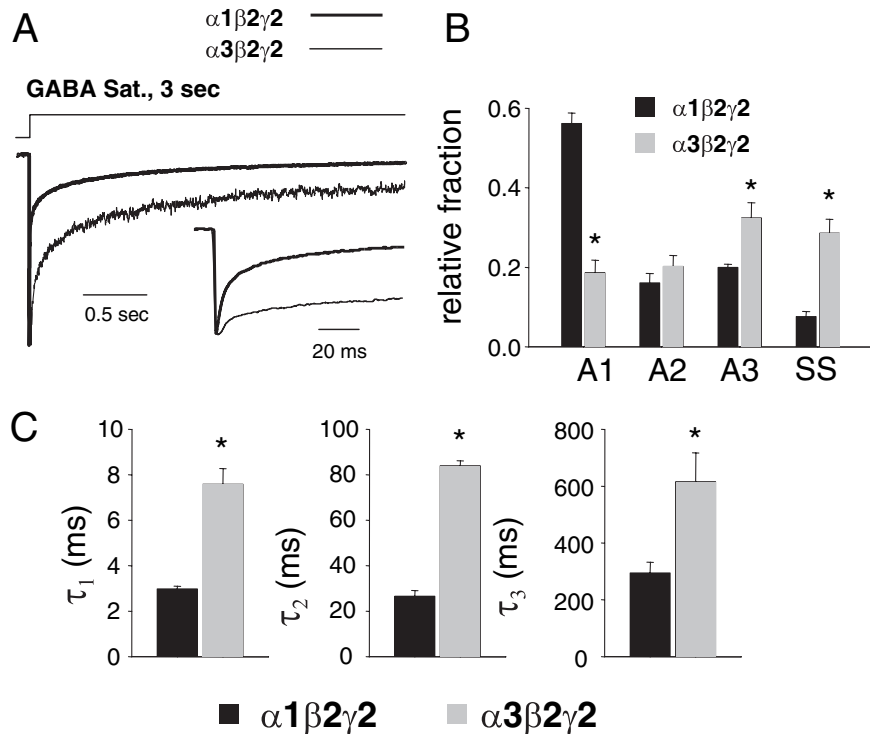


FIG. 4. Comparison of desensitization of currents elicited by GABA applications between  $\alpha 1\beta 2\gamma 2$  and  $\alpha 3\beta 2\gamma 2$  channels. (A) Normalized average of five responses induced by 3 s applications of saturating GABA (GABA Sat.) to a patch excised from human embryonic kidney cells expressing  $\alpha 1\beta 2\gamma 2$  (10 mM GABA) and  $\alpha 3\beta 2\gamma 2$  (50 mM GABA) receptors. Average currents are shown superimposed with a thick line illustrating current from  $\alpha 1\beta 2\gamma 2$  receptors and a thin line illustrating that from  $\alpha 3\beta 2\gamma 2$  receptors. The initial phase of the GABA currents is shown at an expanded scale in an inset at the bottom right. Traces are normalized to the peak amplitude. (B) Summary of the relative contributions of each component to the peak amplitude (A1–A3 and steady-state) of triple exponential curves used to fit the decay of  $\alpha 1\beta 2\gamma 2$  and  $\alpha 3\beta 2\gamma 2$  receptor GABA-gated currents to a steady-state value (SS). (C) Each of the three time constants used for the fitting is reported for  $\alpha 1\beta 2\gamma 2$  and  $\alpha 3\beta 2\gamma 2$  receptors. Each bar represents the mean  $\pm$  SEM of three patches for  $\alpha 1\beta 2\gamma 2$  receptors and seven patches for  $\alpha 3\beta 2\gamma 2$  receptors studied per each subunit combination. \* $P < 0.05$  indicates a significant difference between subunits.

a pronounced fast component with respect to  $\alpha 3\beta 2\gamma 2$  (Fig. 4A insert). The fast time constants ( $\tau_1$ ) obtained in  $\alpha 1\beta 2\gamma 2$  and  $\alpha 3\beta 2\gamma 2$  currents were  $2.9 \pm 0.1$  ( $n = 7$ ) and  $7.5 \pm 0.7$  ms ( $n = 7$ ), respectively ( $P < 0.05$ ) and the relative weight of the fast component (A<sub>1</sub>) in  $\alpha 1\beta 2\gamma 2$  was more than three times larger than that observed in  $\alpha 3\beta 2\gamma 2$  ( $0.56 \pm 0.025$ ,  $n = 7$  and  $0.19 \pm 0.03$ ,  $n = 7$ , respectively,  $P < 0.05$ , Fig. 4B). The middle ( $\tau_2$ ) and slow ( $\tau_3$ ) time constants were also much faster in  $\alpha 1\beta 2\gamma 2$  with respect to  $\alpha 3\beta 2\gamma 2$  (Fig. 4C). Moreover, the relative weight of the steady-state component was significantly larger in  $\alpha 3\beta 2\gamma 2$ -mediated currents when compared with the  $\alpha 1\beta 2\gamma 2$  currents ( $0.286 \pm 0.04$ ,  $n = 7$  and  $0.076 \pm 0.013$ ,  $n = 7$  in  $\alpha 3\beta 2\gamma 2$  and  $\alpha 1\beta 2\gamma 2$ , respectively,  $P < 0.05$ , Fig. 4B). These data show that, following prolonged GABA application,  $\alpha 1\beta 2\gamma 2$  receptors are quickly absorbed into the desensitized state(s) (in  $\sim 3$  ms the current is reduced by more than one half). Moreover, a very low steady state to peak ratio in  $\alpha 1\beta 2\gamma 2$ -mediated currents indicates that these receptors are efficiently trapped into the desensitized state(s). In contrast,  $\alpha 3\beta 2\gamma 2$  receptors are characterized by a markedly slower rate and smaller extent of apparent desensitization (Fig. 4). According to the prediction of the model of Jones & Westbrook (1995), a stronger desensitization would favor prolongation of the slow deactivation component. However, the fact that deactivation of  $\alpha 1\beta 2\gamma 2$ -mediated currents is markedly faster than that of  $\alpha 3\beta 2\gamma 2$  receptors (Fig. 3) should not be regarded as a discrepancy as deactivation could be additionally shaped by other rate constants that might differ between considered receptor types. In particular, the impact of desensitization on current deactivation is largely determined

by the rate of the agonist unbinding ( $k_{\text{off}}$ ) that, as suggested by channel burst analysis (see later), is slower in  $\alpha 3\beta 2\gamma 2$  receptors. The combination of slower unbinding and weaker desensitization in  $\alpha 3\beta 2\gamma 2$  receptors is considered in detail in the Model simulations section below. It is likely that these differences in desensitization kinetics underlie, at least partially, faster onset kinetics in  $\alpha 1\beta 2\gamma 2$ -mediated currents evoked by saturating [GABA] (Fig. 2, see also Model simulations section below).

In addition, we studied the kinetics of the current relaxation after a long (3 s) pulse. The deactivation process was markedly slower in  $\alpha 3\beta 2\gamma 2$  with respect to  $\alpha 1\beta 2\gamma 2$  receptors, with weighted time constants of  $743.3 \pm 73.7$  and  $364 \pm 40$  ms, respectively ( $n = 7$ ). These results produce further evidence that the coupling between desensitization and deactivation kinetics is similar in both  $\alpha 1\beta 2\gamma 2$  and  $\alpha 3\beta 2\gamma 2$  receptors.

#### *$\alpha 3\beta 2\gamma 2$ -mediated currents show faster recovery in paired-pulse experiments*

In order to further explore the impact of desensitization and unbinding rate on  $\alpha 1\beta 2\gamma 2$ - and  $\alpha 3\beta 2\gamma 2$ -mediated currents evoked by brief GABA pulses, a standard paired-pulse protocol was employed (pairs of 2 ms applications of saturating [GABA] separated by a variable interpulse interval). A markedly lower amplitude of the second response to GABA shows that even a short (2 ms) agonist pulse results in a dynamic entry into the desensitized states

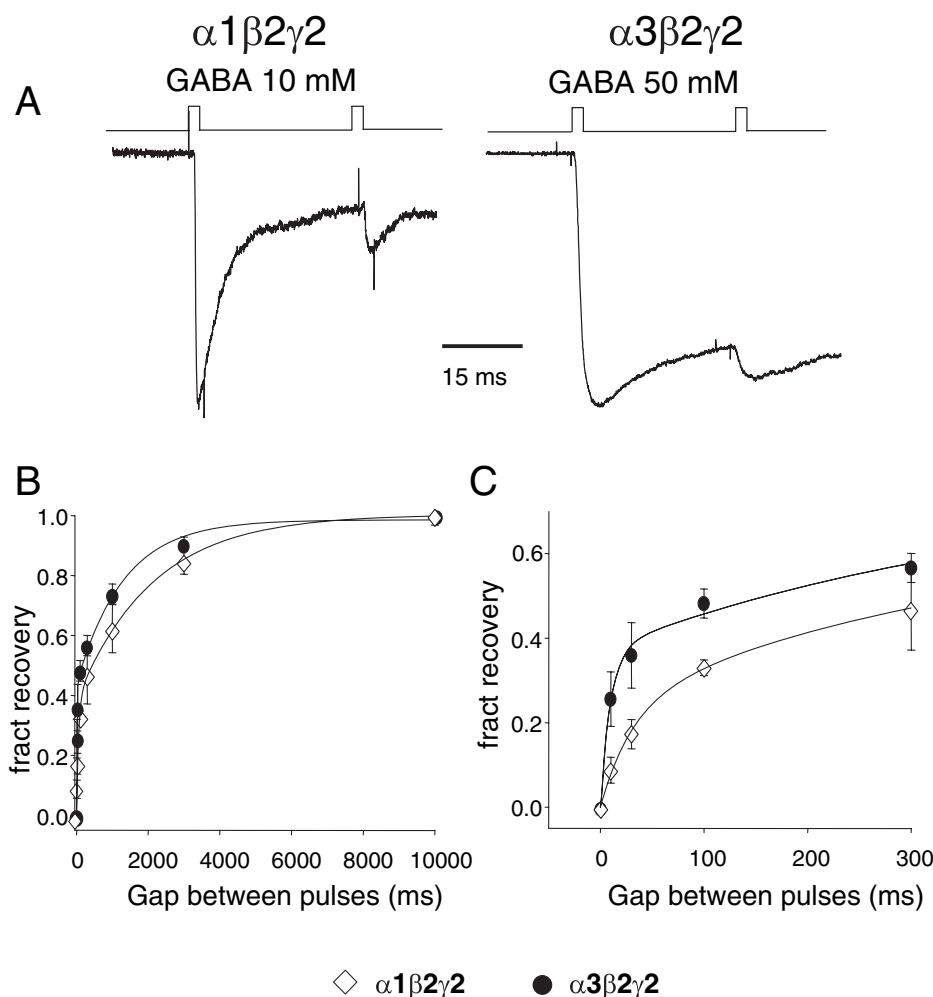


FIG. 5. Recovery process in the paired-pulse experiments differs between  $\alpha 1\beta 2\gamma 2$  and  $\alpha 3\beta 2\gamma 2$  channels. (A) Examples of normalized averages of five traces evoked by two successive applications of 2 ms GABA (10 and 50 mM) pulses separated by 30 ms intervals in a patch excised from human embryonic kidney (HEK) cells expressing  $\alpha 1\beta 2\gamma 2$  (left) and  $\alpha 3\beta 2\gamma 2$  (right) receptors. (B) Comparison of the recovery time course of the second response from desensitization in at least 15 patches excised from HEK cells expressing  $\alpha 1\beta 2\gamma 2$  ( $\diamond$ ) and  $\alpha 3\beta 2\gamma 2$  ( $\bullet$ ) receptors. The percent recovery at each designated separation of two brief GABA pulses is calculated as described in Materials and methods, and plotted against the interpulse interval. Each data point represents the mean  $\pm$  SEM of eight patches studied. (C) The data in B are shown at an expanded time scale to better illustrate the components of the double exponential fitting of the recovery.

of both receptor types (Fig. 5A). Figure 5B and C shows the time course of recovery for  $\alpha 1\beta 2\gamma 2$  and  $\alpha 3\beta 2\gamma 2$  receptors, indicating that this process is considerably faster in the latter. For both receptor types, the time evolution of recovery showed two exponential components. Both fast and slow components were faster in  $\alpha 3\beta 2\gamma 2$  with respect to  $\alpha 1\beta 2\gamma 2$ , although the difference observed in the fast component was more pronounced than that in the slow component ( $\tau_1 = 6.8$  ms,  $\tau_2 = 1836.4$  ms for  $\alpha 3\beta 2\gamma 2$ ,  $n = 6$  and  $\tau_1 = 103.2$  ms,  $\tau_2 = 7642.3$  ms for  $\alpha 1\beta 2\gamma 2$ ,  $n = 5$ , Fig. 5). In contrast, the relative weights of the fast and slow recovery components were similar in the two receptor subtypes ( $A_1 = 0.5$ ,  $A_2 = 0.5$  for  $\alpha 3\beta 2\gamma 2$  and  $A_1 = 0.53$ ,  $A_2 = 0.47$  for  $\alpha 1\beta 2\gamma 2$ , Fig. 5). These data clearly show that the impact of the desensitization process on currents elicited by brief and saturating GABA pulses is much stronger in  $\alpha 1\beta 2\gamma 2$  than in  $\alpha 3\beta 2\gamma 2$  receptors. This finding is consistent with the faster and more profound desensitization of  $\alpha 1\beta 2\gamma 2$  receptors observed in experiments in which prolonged and saturating [GABA] pulses were applied (Fig. 4). However, at present, it is difficult to precisely estimate to what extent a faster recovery and a smaller rate and extent of desensitization of  $\alpha 3\beta 2\gamma 2$  receptors are a

consequence of a slower entry into the desensitized conformation(s) or of a faster exit from this state(s). In particular, it should be borne in mind that faster recovery in the paired-pulse experiments (Fig. 5) does not necessarily reflect a faster resensitization rate (transition rate from desensitized to closed state) as the recovery process is known to critically depend also on unbinding and on the desensitization rate (Jones & Westbrook, 1995; Mozrzymas *et al.*, 2003a).

Additional important information coming from paired-pulse experiments is the presence of a very slow recovery component in both  $\alpha 1\beta 2\gamma 2$  and  $\alpha 3\beta 2\gamma 2$  receptors ( $\sim 8$  and 2 s, respectively). Although slow ( $\tau \sim 10$  s) desensitized states have already been described for GABA<sub>A</sub>Rs, especially in experiments in which long pulses of GABA were applied (e.g. Mozrzymas & Cherubini, 1998; Hutcheon *et al.*, 2000; Overstreet *et al.*, 2000), it is commonly believed that such a long-lasting desensitization component is unlikely to play any important role in shaping currents evoked by brief agonist pulses. In contrast, our data provide evidence that a GABA pulse as short as 2 ms is sufficient to induce conformational transitions towards desensitized states living for several seconds.

*$\alpha 1\beta 2\gamma 2$  and  $\alpha 3\beta 2\gamma 2$  receptors show similar opening/closing kinetics but differ in burst duration*

As stated above, the rise time of currents evoked by saturating concentrations of GABA may depend on both opening/closing and desensitized state(s) but a direct estimation of contributions of these conformational transitions is not straightforward. In order to address this issue, gating properties of these two receptor subtypes were studied at the single-channel level. By analysing the intraburst kinetics it is possible to extract information about the kinetics of the open/closed transitions. Within a burst, in fact, the receptor is believed to experience fast transitions between open/closed states prior to unbinding of the agonist or entering into long-living non-conductive states (e.g. desensitized states). Single-channel currents were recorded (Fig. 6A) from excised patches continuously exposed to GABA-containing solution (100 and 600  $\mu\text{M}$  for  $\alpha 1\beta 2\gamma 2$  and  $\alpha 3\beta 2\gamma 2$  receptors, respectively). These concentrations are considerably above the  $\text{EC}_{50}$  values for these receptors (Verdoorn, 1994; Gingrich *et al.*, 1995) and it is therefore expected that the single-channel activity mainly reflects the transitions between fully-bound conformations. The single-channel conductance was the same for  $\alpha 1\beta 2\gamma 2$  and  $\alpha 3\beta 2\gamma 2$  ( $27.7 \pm 0.8$  and  $27.1 \pm 0.6$  pS, respectively,  $n = 5$ , Fig. 6C). Openings at subconductance levels were observed in both  $\alpha 1\beta 2\gamma 2$  and  $\alpha 3\beta 2\gamma 2$  receptors but their occurrence was less than 1% of the total openings and they were discarded from the analysis. The intraburst open time distributions obtained from both  $\alpha 1\beta 2\gamma 2$ - and  $\alpha 3\beta 2\gamma 2$ -mediated single-channel currents were best fitted by two exponential probability density functions and, interestingly, the time constants together with respective percentages and mean open time found for  $\alpha 1\beta 2\gamma 2$  receptors were indistinguishable from those observed for  $\alpha 3\beta 2\gamma 2$  receptors (Fig. 6C). As detailed in Materials and methods, the critical end-burst closed time was calculated from the analysis of closed time distributions. For both receptor types, a sum of up to five exponential functions was used to fit these distributions well. For both  $\alpha 1\beta 2\gamma 2$  and  $\alpha 3\beta 2\gamma 2$  receptors, the values of the two shortest time constants showed small cell-to-cell variability and were interpreted as intraburst closures, whereas the slowest time constant was variable and strongly depended on the number of channels present in the patch and probably represented closed (or desensitized) periods between bursts. No significant difference was found when comparing the two shortest closed time constants for  $\alpha 3\beta 2\gamma 2$  channels with those determined for  $\alpha 1\beta 2\gamma 2$  receptors ( $\tau_1 = 0.45 \pm 0.035$  ms and  $\tau_2 = 2.09 \pm 0.052$  ms compared with  $\tau_1 = 0.49 \pm 0.03$  ms and  $\tau_2 = 2.62 \pm 0.36$  ms for  $\alpha 1\beta 2\gamma 2$  and  $\alpha 3\beta 2\gamma 2$  receptors, respectively;  $P > 0.05$ , each measurement made for at least  $n = 10$  patches). The lack of significant difference in either open or closed times within bursts indicates that the opening/closing kinetics of  $\alpha 1\beta 2\gamma 2$  and  $\alpha 3\beta 2\gamma 2$  receptors do not differ.

In the same recordings for which open and closed distributions were determined, burst analysis was additionally performed for both receptor types (Fig. 6B). As shown in Fig. 6D,  $\alpha 3\beta 2\gamma 2$  receptors showed significantly longer bursts than  $\alpha 1\beta 2\gamma 2$  receptors. In particular, the averaged burst duration was nearly 60% longer for  $\alpha 3\beta 2\gamma 2$  receptors and this difference was associated with both a considerably larger slow burst time constant and its percentage in these receptors (Fig. 6D). No significant differences were found between the respective time constants of the fast components of burst distributions.

To obtain a further link between information from macroscopic currents (such as, e.g. in Figs 1–5) and single-channel currents, patches with low number of channels were used for single-channel recordings (Fig. 7A and B) when applying the protocol depicted in

Fig. 3 to record the deactivation kinetics (2 ms pulse of saturating [GABA]). Figure 7B illustrates a more typical occurrence of GABA responses in multichannel patches. Although the large number of channels prevented a detailed analysis, it was clear that patches from  $\alpha 3\beta 2\gamma 2$  receptors expressing human embryonic kidney cells were endowed with more frequent late openings. In patches with a small number of channels, the mean open times of  $\alpha 1\beta 2\gamma 2$  and  $\alpha 3\beta 2\gamma 2$  receptors, determined for 4 s time windows, were not significantly different ( $1.42 \pm 0.05$  ms,  $n = 6$  and  $1.57 \pm 0.07$  ms,  $n = 7$ ). When analysing the entire trace after GABA applications, the mean burst duration was longer for  $\alpha 3\beta 2\gamma 2$  receptors (Fig. 7D), similar to that observed in steady-state conditions (Fig. 6). However, in both receptor types the burst duration measured in the considered non-equilibrium conditions was clearly shorter than those obtained in the steady-state (compare Figs 6D and 7C and D). This difference is likely to reflect the fact that upon deactivation burst can be terminated not only by entrance into a bound non-conductive state but additionally by dissociating the agonist. However, the vast majority of our recordings were collected from multichannel patches and therefore precise assessment of the impact of these two mechanisms is not possible. To further address this issue, the single-channel analysis was performed for three arbitrarily defined epochs: 0–500, 500–1000 and >1000 ms after brief GABA application. As shown in Fig. 7D, in both  $\alpha 1\beta 2\gamma 2$  and  $\alpha 3\beta 2\gamma 2$  receptors the mean burst duration is clearly decreasing in successive epochs, further indicating that the relative proportion of brief events is increasing during late phases of deactivation. The last finding may also suggest an increased proportion of short-living singly-bound open states in the late epochs (Macdonald *et al.*, 1989).

Taking advantage of single-channel recordings, we compared the frequency of late single-channel openings of  $\alpha 1\beta 2\gamma 2$  and  $\alpha 3\beta 2\gamma 2$  receptors in the third epoch (1000–4000 ms). The frequency of late openings was normalized to the  $N_p$  value at peak (where  $N$  is number of channels and  $p$  is open probability at peak,  $N_p$  was calculated as the ratio of peak current and single-channel current). As shown in Fig. 7E, the frequency of late openings was much larger in  $\alpha 3\beta 2\gamma 2$  receptors. The original model of Jones & Westbrook (1995) predicts that strongly absorbing desensitized states should favor late single-channel openings. In  $\alpha 1\beta 2\gamma 2$  receptors, both the rate and extent of desensitization were particularly strong. In this situation, late openings, following sojourns in strongly absorbing desensitized state(s), could be scattered over a long period of time yielding an undetectable contribution to the macroscopic currents. Alternatively, fully-bound receptor in the desensitized state might dissociate the agonist molecule thus reducing the duration of deactivation and the probability of late openings due to interruption of ‘oscillation’ between fully-bound desensitized, closed and open states. These possibilities are further investigated in the next section.

### Model simulations

The data collected here indicate that functional differences between  $\alpha 1$ - and  $\alpha 3$ -containing  $\text{GABA}_A\text{Rs}$  lie in both ligand-binding properties (affinity) and in the kinetics of conformational transitions between bound states (gating). However, the major difficulty in assessing the contribution of any particular transition rate is that the time course of the measured currents reflects a complex process that is potentially shaped by all of the conformational transitions functionally coupled to each other (Colquhoun, 1998; Mozrzymas *et al.*, 2003a). In particular, knowledge of the affinity coefficient alone, in non-stationary conditions, is of limited usefulness as binding and unbinding rates might



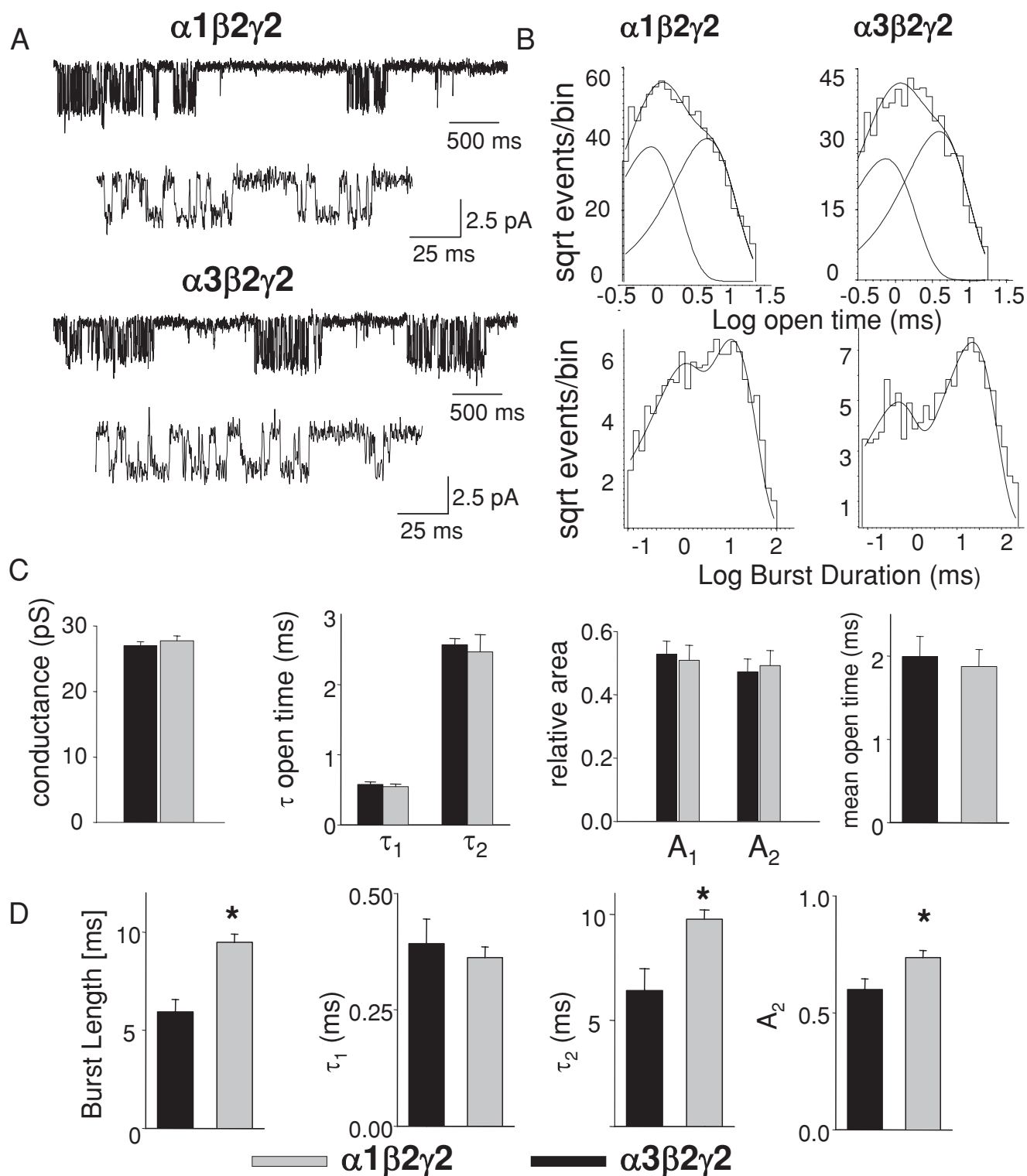


FIG. 6. Comparison between  $\alpha 1\beta 2\gamma 2$  and  $\alpha 3\beta 2\gamma 2$  GABA-channel currents elicited by long-lasting GABA application. (A) Channel activity evoked by long-lasting applications of GABA to outside-out patches excised from human embryonic kidney (HEK) cells expressing  $\alpha 1\beta 2\gamma 2$  (top, 100  $\mu\text{M}$  GABA) and  $\alpha 3\beta 2\gamma 2$  (bottom, 600  $\mu\text{M}$  GABA) receptors (holding potential,  $-100$  mV). Inset: a fraction of the single-channel current activity at an expanded time scale. Corresponding calibration bars are shown in the lower right corner of traces. (B) Distribution of open time (top) and burst durations (bottom) for the patches in A. Distributions are fitted with a double exponential function. (C) Summary of chord conductance and open times characterizing the main conductance state of single-channel current in at least 10 patches excised from HEK cells expressing  $\alpha 1\beta 2\gamma 2$  and  $\alpha 3\beta 2\gamma 2$  receptors. (D) A comparison of average burst length of  $\alpha 1\beta 2\gamma 2$  and  $\alpha 3\beta 2\gamma 2$  channels in these patches and the parameters ( $A_2$ ,  $\tau_1$  and  $\tau_2$ ) from double exponential fitting of burst duration distributions as in B. \* $P < 0.05$  indicates a significant difference between subunits.

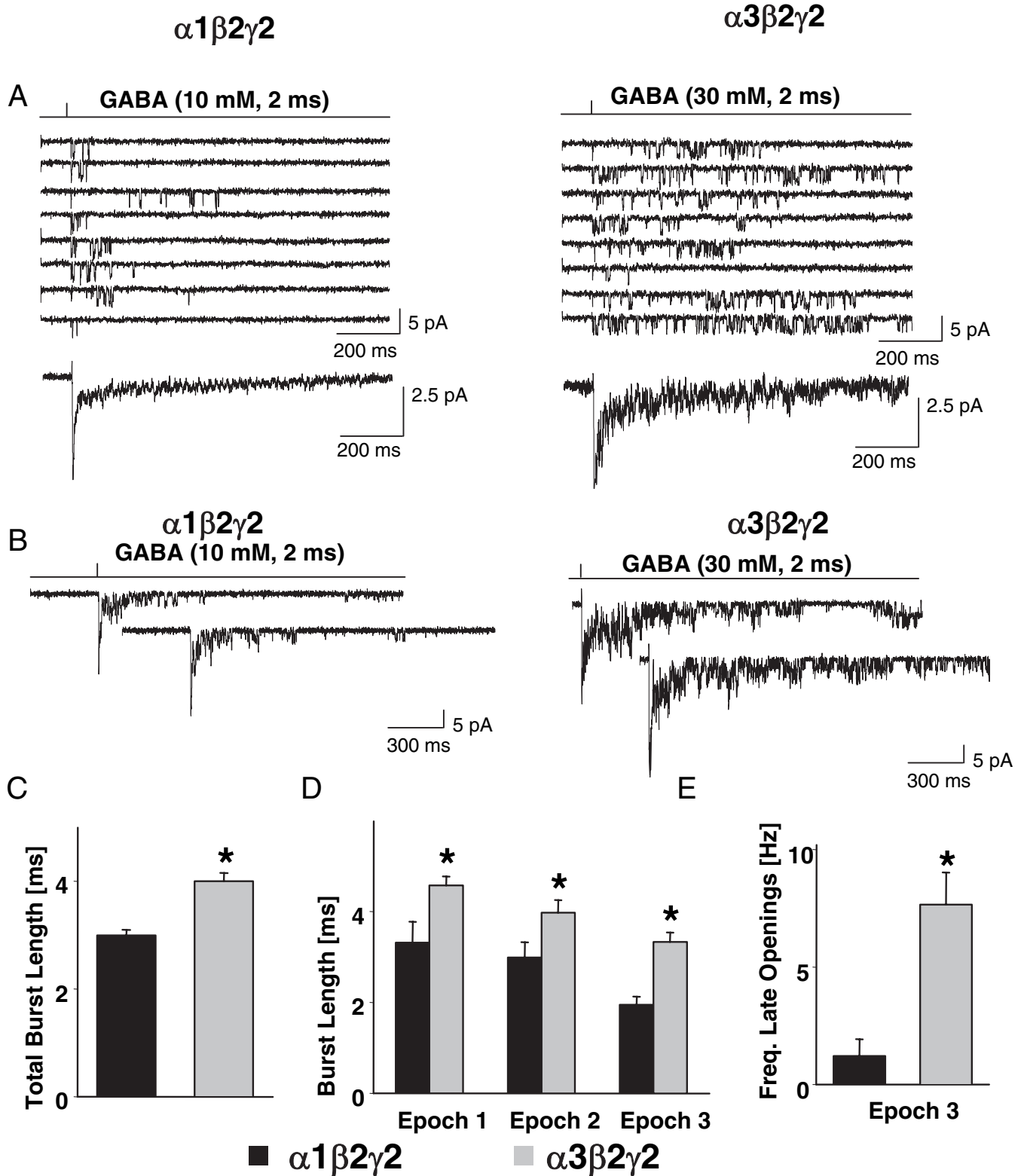


FIG. 7. Comparison between  $\alpha 1\beta 2\gamma 2$  and  $\alpha 3\beta 2\gamma 2$  GABA-channel currents elicited by brief GABA applications. (A) Multiple records of 1 s illustrating channel activity evoked by 2 ms applications of GABA to outside-out patches in two patches excised from human embryonic kidney (HEK) cells expressing single  $\alpha 1\beta 2\gamma 2$  (left, 10 mM GABA) and  $\alpha 3\beta 2\gamma 2$  (right, 30 mM GABA) channels (holding potential,  $-100$  mV). The mean current resulting from the average of the single-channel records is shown in the bottom trace (right and left panel). (B) Two records of 2 s illustrating channel activity evoked by 2 ms applications of GABA to outside-out patches in two patches excised from HEK cells expressing many  $\alpha 1\beta 2\gamma 2$  (top, 10 mM GABA) and  $\alpha 3\beta 2\gamma 2$  (bottom, 30 mM GABA) channels (holding potential,  $-100$  mV). Individual channel activity is visible in the tail of these currents. (C) Comparison of mean burst length for  $\alpha 3\beta 2\gamma 2$  and  $\alpha 1\beta 2\gamma 2$  channels measured during the entire recording period (4 s). (D) Comparison of mean burst lengths in three epochs: 0–500 ms (Epoch 1), 500–1000 ms (Epoch 2) and >1000 ms (Epoch 3). Note that burst durations tend to decrease with time after applications. (E) Comparison of frequencies of late openings (in Epoch 3) for  $\alpha 1\beta 2\gamma 2$  and  $\alpha 3\beta 2\gamma 2$  receptors. Note that frequency of late openings is several times larger in  $\alpha 3\beta 2\gamma 2$  receptors. \* $P < 0.05$  indicates a significant difference between subunits.

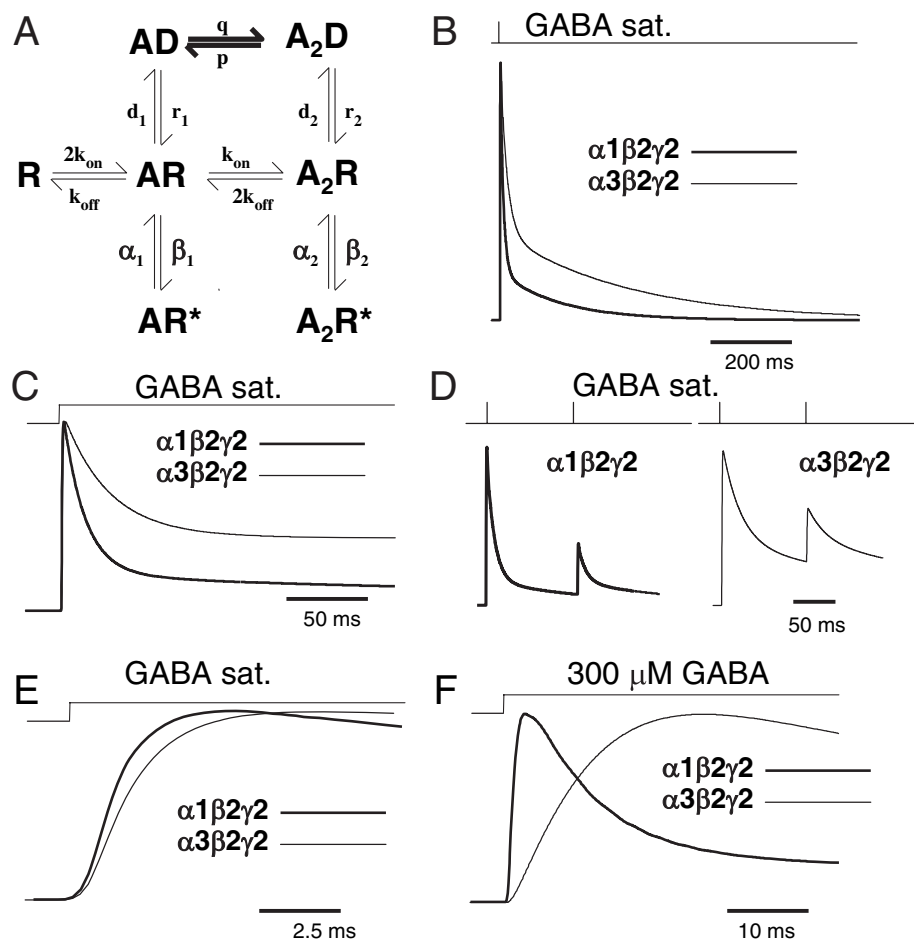


FIG. 8. Model simulations of  $\alpha 1\beta 2\gamma 2$  and  $\alpha 3\beta 2\gamma 2$  receptor-mediated currents. (A) Model of GABA<sub>A</sub> receptor gating (Jones *et al.*, 1998). Thick arrows depict binding and unbinding transitions between singly- and doubly-bound desensitized states. These transitions were found to play an important role in shaping currents mediated by these receptors (see Model Simulations and Discussion). Simulations were performed for the following rate constants for  $\alpha 1\beta 2\gamma 2$  receptor:  $k_{on} = 3.0$ /ms/mM,  $k_{off} = 0.1$ /ms,  $d_2 = 1.5$ /ms,  $r_2 = 0.02$ /ms,  $\beta_2 = 2.5$ /ms,  $\alpha_2 = 0.284$ /ms,  $q = 0.1$ /ms/mM,  $p = 0.005$ /ms,  $d_1 = 0.013$ /ms,  $r_1 = 0.00013$ /ms,  $\beta_1 = 0.2$ /ms,  $\alpha_1 = 1.11$ /ms and for  $\alpha 3\beta 2\gamma 2$  receptor:  $k_{on} = 0.3$ /ms/mM,  $k_{off} = 0.045$ /ms,  $d_2 = 0.3$ /ms,  $r_2 = 0.02$ /ms,  $\beta_2 = 2.5$ /ms,  $\alpha_2 = 0.284$ /ms,  $q = 0.00087$ /ms/mM,  $p = 0.00013$ /ms,  $d_1 = 0.013$ /ms,  $r_1 = 0.00013$ /ms,  $\beta_1 = 0.2$ /ms,  $\alpha_1 = 1.11$ /ms. In B–F, currents simulated for  $\alpha 1\beta 2\gamma 2$  receptors are drawn with a thin line and those for  $\alpha 3\beta 2\gamma 2$  channels with a thick line. In all graphs currents are normalized. (B) Simulations of current responses to brief (2 ms) applications of saturating [GABA]. A slower deactivation for  $\alpha 3\beta 2\gamma 2$  receptors is well reproduced (compare with Fig. 3). (C) Simulated current responses to prolonged application of saturating [GABA]. A smaller rate and extent of apparent desensitization in  $\alpha 3\beta 2\gamma 2$  receptor-mediated currents is well reproduced (compare with Fig. 4). (D) Simulated currents elicited using paired-pulse protocol (pair of 2 ms pulses of saturating [GABA] separated by a 75 ms gap) for  $\alpha 1\beta 2\gamma 2$  (left) and  $\alpha 3\beta 2\gamma 2$  (right) receptors. A larger recovery of the second pulse for  $\alpha 3\beta 2\gamma 2$  receptors is properly reproduced (compare with Fig. 5). (E) Simulation of the rising phases of currents elicited by saturating [GABA]. A slower onset rate for  $\alpha 3\beta 2\gamma 2$  receptors is correctly reproduced (compare with Fig. 2). (F) Simulations of current responses to a non-saturating GABA concentration (300  $\mu M$ ). A dramatically slower onset of currents mediated by  $\alpha 3\beta 2\gamma 2$  receptors properly reproduces the experimental findings (compare with Fig. 1).

shape different kinetic characteristics of GABAergic currents (Jones *et al.*, 1998). For instance, when considering the responses to brief applications of GABA (e.g. synaptic currents), the binding rate would determine the proportion of GABA<sub>A</sub>Rs that become bound during exposure to the agonist, whereas the unbinding rate would play a crucial role in shaping the current deactivation. Moreover, the time course of GABA-evoked currents depends on the transition rates between bound conformations of the receptor (closed, open and desensitized states). Taking this into account, model simulations were used to explore the differences in binding and gating properties of  $\alpha 1$ - and  $\alpha 3$ -containing GABA<sub>A</sub>Rs. For this purpose, we used a model based on that of Jones & Westbrook (1995). This model, assuming sequential binding of two agonist molecules and opening/desensitization originating from the closed bound state, although simplified, is known to reasonably reproduce the basic properties of GABA<sub>A</sub>R

gating (Jones & Westbrook, 1995; Mozrzymas *et al.*, 2003a,b). Moreover, the fact that deactivation mediated by  $\alpha 1\beta 2\gamma 2$  and  $\alpha 3\beta 2\gamma 2$  receptors shows a similar desensitization/deactivation coupling suggests that the gating schemes of these receptors share major common features. Thus, as a starting point we adapted this model to reproduce the basic kinetic properties of  $\alpha 1\beta 2\gamma 2$  receptors and, secondly, we made an attempt to introduce a minimum of modifications in the respective rate constants to explore the major kinetic differences between  $\alpha 1\beta 2\gamma 2$  and  $\alpha 3\beta 2\gamma 2$  receptors. The rate constants used for description of the  $\alpha 1\beta 2\gamma 2$  receptor kinetics were manually selected to best reproduce the kinetic behavior of these receptors in all considered experimental protocols. The most apparent difference between  $\alpha 1\beta 2\gamma 2$  and  $\alpha 3\beta 2\gamma 2$  receptors was a dramatically slower current onset of responses elicited by non-saturating [GABA] in the case of  $\alpha 3\beta 2\gamma 2$  receptors (Fig. 1), suggesting a substantially lower

value of the association rate constant  $k_{on}$ . Moreover, both the rate and extent of desensitization were markedly smaller in the case of  $\alpha 3\beta 2\gamma 2$  receptors (Fig. 4), suggesting a smaller desensitization ( $d_2$ ) and/or a faster resensitization ( $r_2$ ) rate. Similarly, a faster recovery in the paired-pulse experiments of  $\alpha 3$  subunit-containing receptors (Fig. 5) suggests smaller desensitization and resensitization rates ( $d_2$  and  $r_2$ ) in  $\alpha 3\beta 2\gamma 2$  receptors. However, the recovery process may additionally depend on the unbinding rate  $k_{off}$  (Jones & Westbrook, 1995; Mozrzymas *et al.*, 2003a). The onset rate of current responses to saturating GABA is slower for  $\alpha 3\beta 2\gamma 2$  receptors than for  $\alpha 1\beta 2\gamma 2$  receptors indicating a difference in kinetics of fully-bound conformational transitions. However, as already mentioned, this feature potentially depends not only on the opening/closing rates but also on the desensitization kinetics (Mozrzymas *et al.*, 2003a).

The most striking feature of the  $\alpha 3\beta 2\gamma 2$  receptor is that, in spite of its lower apparent affinity (with respect to  $\alpha 1\beta 2\gamma 2$ ), the deactivation of currents mediated by these receptors is much slower than that of  $\alpha 1\beta 2\gamma 2$  GABA<sub>A</sub>Rs. Moreover, as mentioned above, such a slow deactivation is associated with a relatively weak desensitization in comparison to  $\alpha 1\beta 2\gamma 2$  receptors.

The lack of difference in the single channel open and closed time distributions for  $\alpha 1\beta 2\gamma 2$  and  $\alpha 3\beta 2\gamma 2$  receptors indicates that the rate constants governing transitions between fully-bound open and closed states ( $\beta_2$  and  $\alpha_2$ ) are not substantially different.

Taking into account these results, we made an attempt to reproduce the major kinetic differences between the  $\alpha 1\beta 2\gamma 2$  and  $\alpha 3\beta 2\gamma 2$  GABA<sub>A</sub>Rs by manipulating  $k_{on}$ ,  $k_{off}$ ,  $d_2$  and  $r_2$  rate constants. As expected, a decrease in the binding rate  $k_{on}$  was sufficient to reproduce a slower onset of responses to non-saturating [GABA]. Moreover, a reduction in the  $d_2$  rate constant alone allowed reproduction of a decrease in the rate and extent of desensitization as well as the acceleration of the recovery process in the double-pulse protocol (Figs 4 and 5). However, the reproduction of remarkably slower deactivation of currents mediated by  $\alpha 3\beta 2\gamma 2$  receptors (Fig. 1) required setting the unbinding rate considerably slower than for  $\alpha 1\beta 2\gamma 2$  receptors. Additional support for a slower unbinding rate of  $\alpha 3\beta 2\gamma 2$  receptors comes from the analysis of the single-channel currents in the stationary and non-stationary conditions. Although no clear differences were seen in the single open channel distributions (Figs 6 and 7), the considerably longer burst duration observed for  $\alpha 3\beta 2\gamma 2$  might indicate a slower unbinding for this receptor type (Figs 6 and 7).

Based on our experimental findings, in a first set of model simulations using the model of Jones & Westbrook (1995), an attempt was made to reproduce the kinetic behavior of  $\alpha 3\beta 2\gamma 2$  receptors by decreasing  $k_{on}$ ,  $k_{off}$ ,  $d_2$  and  $r_2$  with respect to the respective rate constant used for  $\alpha 1\beta 2\gamma 2$  receptors. The rate constants for  $\alpha 1\beta 2\gamma 2$  receptors were  $k_{on} = 3.0/\text{ms}/\text{mM}$ ,  $k_{off} = 0.03/\text{ms}$ ,  $d_2 = 2/\text{ms}$ ,  $r_2 = 0.02/\text{ms}$ ,  $\beta_2 = 2.5/\text{ms}$ ,  $\alpha_2 = 0.284/\text{ms}$ ,  $d_1 = 0.013/\text{ms}$ ,  $r_1 = 0.00013/\text{ms}$ ;  $\beta_1 = 0.2/\text{ms}$  and  $\alpha_1 = 1.11/\text{ms}$  whereas those for  $\alpha 3\beta 2\gamma 2$  receptors were  $k_{on} = 0.3/\text{ms}/\text{mM}$ ,  $k_{off} = 0.03/\text{ms}$ ,  $d_2 = 0.2/\text{ms}$ ,  $r_2 = 0.015/\text{ms}$ ,  $\beta_2 = 2.5/\text{ms}$ ,  $\alpha_2 = 0.284/\text{ms}$ ,  $d_1 = 0.013/\text{ms}$ ,  $r_1 = 0.00013/\text{ms}$ ,  $\beta_1 = 0.2/\text{ms}$  and  $\alpha_1 = 1.11/\text{ms}$ . Such changes enabled us to qualitatively reproduce all major kinetic differences between responses mediated by  $\alpha 3\beta 2\gamma 2$  and  $\alpha 1\beta 2\gamma 2$  receptors: slower rise time of currents evoked by high (10 mM) and low (10–300  $\mu\text{M}$ ) GABA concentrations, slower deactivation, smaller rate and extent of desensitization, and accelerated recovery from desensitization in the case of the former (data not shown). However, manipulations of the  $k_{on}$ ,  $k_{off}$ ,  $d_2$  and  $r_2$  rate constants (assuming other rate constants equal) turned out to be insufficient to assure adequate quantitative reproduction of our experimental data. In general, the major difficulty was to

concomitantly reproduce a substantial slower deactivation together with faster recovery in paired-pulse experiments for  $\alpha 3\beta 2\gamma 2$  with respect to  $\alpha 1\beta 2\gamma 2$  (Figs 3 and 5). Taking this into account we made an attempt to consider some parsimonious explanations for this discrepancy. As stated above, the desensitization of  $\alpha 1\beta 2\gamma 2$  receptors is much stronger than that of  $\alpha 3\beta 2\gamma 2$  receptors (Figs 4 and 5). Such a strongly absorbing desensitized state as that of  $\alpha 1\beta 2\gamma 2$  receptor is expected to favor a slow deactivation and the appearance of late single-channel openings following a brief application of saturating GABA pulse (see Fig. 7 for examples of late openings). However, as shown in Figs 3 and 7, the deactivation is slower and the occurrence of late openings is considerably more frequent for  $\alpha 3\beta 2\gamma 2$  receptors. An intuitive explanation for this observation is that  $\alpha 1\beta 2\gamma 2$  receptors might exit from desensitization at an extremely slow and therefore undetectable rate, a behavior theoretically predictable by the model of Jones & Westbrook (1995). Alternatively, it could be speculated that  $\alpha 1\beta 2\gamma 2$  receptors might have a higher tendency to dissociate the agonist during a sojourn in the fully-bound desensitized state than the  $\alpha 3\beta 2\gamma 2$  receptors. The possibility of agonist binding and unbinding directly from desensitized states has been previously applied in the revised model proposed by Jones *et al.* (1998). One could consider unbinding from the fully-bound open state but such transition would affect open and closed time distributions. Similarly, open and closed time distributions could be affected by the desensitized state originating from the fully-bound conformation, although the presence of a very slow desensitized state cannot be excluded. We therefore have tested the impact of such additional transitions with our simulation (Fig. 8A) and assumed that the proportions between binding and unbinding for desensitized states roughly follow the pattern of binding and unbinding between closed states (i.e. binding is much faster in the case of  $\alpha 1\beta 2\gamma 2$  and unbinding is slower for  $\alpha 3\beta 2\gamma 2$  receptors). Addition of the transitions between singly- and doubly-bound desensitized states produced an acceleration of the slow deactivation component, and resulted in better reproduction of the experimental data. Clearly, dissociation of the agonist during the deactivation phase (in the absence of free agonist) precludes the receptor from visiting the long-living open conformation. Thus, inclusion of agonist binding and unbinding from the desensitized states with the assumption that unbinding is faster in the case of  $\alpha 1\beta 2\gamma 2$  receptors allowed to reproduce more accurately, with respect to the model presented above, all major differences between the  $\alpha 1$  and  $\alpha 3$  subunit-containing GABA<sub>A</sub>Rs (Fig. 8B–F, Table 1). It has to be stressed, however, that the presence of such transitions between desensitized states is only indirectly suggested by the experimental evidence and therefore their actual occurrence remains speculative.

Altogether, our simulation reproduced the major kinetic differences between  $\alpha 3\beta 2\gamma 2$  and  $\alpha 1\beta 2\gamma 2$  receptors with the following minimum requirements: slower binding ( $k_{on}$ ), unbinding ( $k_{off}$ ), desensitization ( $d_2$ ) and resensitization ( $r_2$ ) rates for  $\alpha 3\beta 2\gamma 2$  receptors. In addition, we speculate that the agonist can bind and unbind from the receptor in the desensitized state and, similarly as in the case of the closed state, both binding ( $q$ ) and unbinding ( $p$ ) are slower in the case of  $\alpha 3\beta 2\gamma 2$  receptors.

## Discussion

In the present work we investigated the mechanisms underlying the different kinetic behavior of  $\alpha 1\beta 2\gamma 2$  and  $\alpha 3\beta 2\gamma 2$  GABA<sub>A</sub>Rs. The crucial finding of this study is that these receptors are characterized by profoundly different desensitization kinetics and that this difference has a strong impact on current kinetics mediated by these

TABLE 1. Comparison of simulated data: frame models of Jones & Westbrook (1995) and Jones *et al.* (1998) with the experimental data here

	Rise time at 10 mM (ms)	Deactivation $\tau_w$ (ms)	Desensitization (steady-state : peak)	Paired-pulses recovery (gap 100 ms)	Residuals
$\alpha 1\beta 2\gamma 2$ frame model of Jones & Westbrook (1995)	0.39	31.3	0.16	0.41	0.0022
$\alpha 1\beta 2\gamma 2$ frame model of Jones <i>et al.</i> (1998)	0.40	35.1	0.19	0.32	0.0019
$\alpha 1\beta 2\gamma 2$ experimental data	$0.29 \pm 0.02$	$52.5 \pm 2.9$	$0.21 \pm 0.02$	$0.33 \pm 0.03$	–
$\alpha 3\beta 2\gamma 2$ frame model of Jones & Westbrook (1995)	1.18	139.5	0.46	0.6	0.0097
$\alpha 3\beta 2\gamma 2$ frame model of Jones <i>et al.</i> (1998)	1.19	160.0	0.48	0.46	0.0027
$\alpha 3\beta 2\gamma 2$ experimental data	$1.01 \pm 0.08$	$185.0 \pm 30.0$	$0.53 \pm 0.07$	$0.48 \pm 0.05$	–

Simulated values obtained using both the model frames of Jones & Westbrook (1995) and Jones *et al.* (1998) are compared with the experimental data for four  $\alpha 1\beta 2\gamma 2$  and  $\alpha 3\beta 2\gamma 2$  critical protocols: (i) 10–90% rise time measured at 10 mM GABA; (ii) deactivation kinetics (weighted time constant); (iii) desensitization steady-state : peak ratio (measured at 200 ms) and (iv) fractional recovery in paired-pulse experiments (gap 100 ms). The normalized residuals (see Materials and methods) show that the model frame of Jones *et al.* (1998) provided a better reproduction of our experimental data.

channels. We confirm that  $\alpha 3\beta 2\gamma 2$  receptors are characterized by a peculiar pattern of interaction with agonist characterized by extremely slow binding and slow unbinding (Gingrich *et al.*, 1995). Single-channel analysis provided evidence that the opening/closing kinetics of  $\alpha 1\beta 2\gamma 2$  and  $\alpha 3\beta 2\gamma 2$  receptors are not significantly different. This information considerably reduced the number of degrees of freedom in our attempts to express kinetic differences between these receptors in terms of receptor gating. However, in both steady-state and non-equilibrium conditions (Figs 6 and 7), the burst durations were longer in  $\alpha 3\beta 2\gamma 2$  than in  $\alpha 1\beta 2\gamma 2$  receptors further suggesting a slower unbinding rate in  $\alpha 3\beta 2\gamma 2$  than in  $\alpha 1\beta 2\gamma 2$  receptors.

In addition, the coupling between desensitization and deactivation kinetics (similar in both  $\alpha 1\beta 2\gamma 2$  and  $\alpha 3\beta 2\gamma 2$  receptors) suggested that the backbone of the kinetic scheme governing the gating of these two receptors might be similar.

The most striking feature of  $\alpha 3\beta 2\gamma 2$  GABA<sub>A</sub>Rs is the combination of a slow deactivation associated with relatively weak desensitization and low apparent affinity. We suggest that, due to the profound and fast desensitization in  $\alpha 1\beta 2\gamma 2$  receptors, most of them would be quickly desensitized (within a few milliseconds) making the overall deactivation process faster than that measured for  $\alpha 3\beta 2\gamma 2$  receptors. Thus, after a fast and massive entry into desensitization, the exit of  $\alpha 1\beta 2\gamma 2$  receptors from this strongly absorbing state would be slow, giving rise to a small and hardly detectable current. In contrast, in  $\alpha 3\beta 2\gamma 2$  receptors a weaker entry in desensitization would partially preclude this mechanism with a consequent slowing down of the deactivation process. This would also explain the less frequent occurrence of late openings in  $\alpha 1\beta 2\gamma 2$  single-channel currents with respect to those of  $\alpha 3\beta 2\gamma 2$ . In  $\alpha 1\beta 2\gamma 2$ , late reopenings of receptors exiting from a slow desensitized state could be scattered over a long period of time, producing undetectable macroscopic currents. This scenario does not contradict the framework of Jones & Westbrook (1995) and actually generalizes their theory by pointing out that the proposed slowing down of deactivation by desensitization is true only in a defined range of desensitization/resensitization and unbinding rate constant values.

Our data indicate that the change of binding/unbinding and desensitization onset is a minimum requirement to reproduce the observed different kinetic pattern in  $\alpha 1\beta 2\gamma 2$ - and  $\alpha 3\beta 2\gamma 2$ -mediated currents. Nevertheless, by keeping the structure proposed by Jones & Westbrook (1995) only a qualitative reproduction of the experimental data could be achieved. This leaves room for further speculation about the differences in gating of these two receptor subtypes. Thus, in an attempt to improve the formal fit with our experimental data, as detailed in the Model simulations section above, we assume, as a matter of speculation, transitions between singly- and doubly-bound

desensitized states (designated by thick arrows in the model in Fig. 8A). These transitions were previously proposed in a revision of their model by Jones *et al.* (1998) but the p and q rate constants were considerably smaller than those estimated from our results in the present study. It is of note that the presence of these transitions might affect the frequency of late openings; for the late single-channel openings after brief application of saturating [GABA], fully-bound desensitized receptors, instead of returning to the doubly-bound closed state, might unbind the agonist molecule and return (possibly via singly-bound open conformation) to the closed unbound conformation. We therefore suggest that multiple sojourns in the desensitized closed and open states prior to unbinding of the agonist (Jones & Westbrook, 1995) set the upper limit for the duration of deactivation whereas unbinding from the fully-bound desensitized state shortens this process. Such a shortening would be more efficient for  $\alpha 1\beta 2\gamma 2$  than for  $\alpha 3\beta 2\gamma 2$  channels because of stronger accumulation in the desensitized state (due to a markedly larger desensitization rate with the same resensitization rate, see Model simulations section above) and faster unbinding from the desensitized state in  $\alpha 1\beta 2\gamma 2$  receptors. Chang *et al.* (2002) provided direct evidence for unbinding from the bound desensitized state of recombinant  $\alpha 1\beta 2\gamma 2$  receptors, expressed in *Xenopus* oocytes, by measuring [<sup>3</sup>H]GABA release. However, the resolution of the binding measurements applied in their experiments allowed the consideration of only very slow desensitization processes (in the range of several seconds) and therefore a direct qualitative comparison to our data is not possible. It is worth emphasizing that, due to transitions between bound desensitized states combined with sufficiently fast unbinding, an increase in the rate and extent of desensitization might correlate with an acceleration of deactivation kinetics, contrary to the prediction of the original model of Jones & Westbrook (1995).

As discussed above, consideration of binding and unbinding between singly- and doubly-bound desensitized states improved the fit of our data. We cannot exclude, however, that additional transitions could take place. For instance, although several additional possibilities are offered by allosteric models (e.g. Scheller & Forman, 2002; Rusch & Forman, 2005) in which many extra transitions are allowed (e.g. between fully-bound open and desensitized states), these transitions did not appear essential to explain our major observations.

Our data further underscore specific roles played by binding and unbinding rates in shaping the current responses in non-equilibrium conditions (Jones *et al.*, 1998). A receptor with the same affinity as the  $\alpha 3\beta 2\gamma 2$  channel but with faster binding and unbinding would give rise to a profoundly different time course of current responses. A key feature of the  $\alpha 3\beta 2\gamma 2$  receptor is an extremely slow unbinding rate that favors multiple sojourns of the receptor in the fully-bound states. As desensitization of this receptor is weaker than in  $\alpha 1\beta 2\gamma 2$  channels,

there is a higher probability of multiple entrances into the open state in  $\alpha 3\beta 2\gamma 2$  receptors. Moreover, as already mentioned, the slower unbinding rate gives rise to longer burst durations in these channels, further increasing the overall open probability for this receptor. The properties of  $\alpha 3\beta 2\gamma 2$  receptors illustrate a very efficient functional coupling between conformational states of the channel (Colquhoun, 1998; Mozrzymas *et al.*, 2003a). Clearly, the channel properties (binding and unbinding) that define the receptor affinity are functionally 'interacting' with transitions between bound states defined as gating and this phenomenon is particularly favored by the slow unbinding rate.

The physiological role of the kinetic differences between  $\alpha 1\beta 2\gamma 2$  and  $\alpha 3\beta 2\gamma 2$  receptors is not clear. Kinetics of deactivation is believed to play a pivotal role in shaping the time course of synaptic currents. Indeed, synaptic GABAergic currents may last as long as hundreds of milliseconds, whereas synaptically released agonist is present within the synaptic cleft for less than 1 ms (Clements, 1996; Mozrzymas, 2004). Fast kinetics of  $\alpha 1\beta 2\gamma 2$  channels suggests that these receptors could be involved in processes requiring high temporal resolution (e.g. rapid synaptic currents participating in coincidence detection), whereas slow  $\alpha 3\beta 2\gamma 2$  channels would be more suitable in phenomena requiring lower temporal precision but a more sustained action. Gao *et al.* (1993) stained neurons in Raphe nuclei with antisera that recognize  $\alpha 1$  and  $\alpha 3$  subunits, and found that the vast majority of serotonergic neurons expressed the  $\alpha 3$  subunit. Browne *et al.* (2001) analysed GABAergic synaptic currents and single-channel kinetics in the reticular nucleus and ventrobasal complex, and attributed the observed differences to differential expression of  $\alpha 1$  and  $\alpha 3$  subunits in these brain areas. More recently, Yee *et al.* (2005) investigated  $\alpha 3$  knockout mice and found that the lack of GABA<sub>A</sub>Rs containing this subunit was associated with a hyperdopaminergic phenotype, similar to that observed in schizophrenia. It may be hypothesized that slow kinetics of receptors containing  $\alpha 3$  subunits offers some advantages for the physiological role of neurons releasing these monoamines. Interestingly, during development, the expression of the  $\alpha 3$  subunit decreases whereas that of the  $\alpha 1$  subunit increases and this expression pattern is accompanied by a trend of acceleration of GABAergic synaptic currents (for review see Vicini & Ortinski, 2004). Moreover, we have recently found that the synaptic GABA transient in cerebellar interneurons is more robust at early developmental stages (Barberis *et al.*, 2005), thus making the response of synapses containing  $\alpha 3\beta 2\gamma 2$  receptors more effective. The extremely slow binding rate of  $\alpha 3\beta 2\gamma 2$  channels is expected to result in trimming down of the size of the synaptic response due to brief GABA transients and makes these channels better suited to respond only to repetitive synaptic transients such as those occurring with high-frequency stimulation. In conclusion, the kinetic analysis presented here provides evidence that the major differences in  $\alpha 1\beta 2\gamma 2$  and  $\alpha 3\beta 2\gamma 2$  receptor functioning are due to the slower rate and smaller extent of desensitization, and slower binding and unbinding rates. We speculate that such a slower binding/unbinding rate in  $\alpha 3\beta 2\gamma 2$  receptors (with respect to  $\alpha 1\beta 2\gamma 2$ ) may also occur between desensitized states.

## Acknowledgements

Supported by NIMH grant MH64797 and Wellcome Trust International Senior Research Fellowship in Biomedical Science (grant no. 070231/Z/03/Z).

## Abbreviations

GABA<sub>A</sub>R, GABA<sub>A</sub> receptor.

## References

- Barberis, A., Lu, C., Vicini, S. & Mozrzymas, J.W. (2005) Developmental changes of GABA synaptic transient in cerebellar granule cells. *Mol. Pharmacol.*, **67**, 1221–1228.
- Bohme, I., Rabe, H. & Luddens, H. (2004) Four amino acids in the alpha subunits determine the gamma-aminobutyric acid sensitivities of GABA<sub>A</sub> receptor subtypes. *J. Biol. Chem.*, **279**, 35 193–35 200.
- Browne, S.H., Kang, J., Akk, G., Chiang, L.W., Schulman, H., Huguenard, J.R. & Prince, D.A. (2001) Kinetic and pharmacological properties of GABA<sub>A</sub> receptors in single thalamic neurons and GABA<sub>A</sub> subunit expression. *J. Neurophysiol.*, **86**, 2312–2322.
- Chang, Y., Ghansah, E., Chen, Y., Ye, J., Weiss, D.S. & Chang, Y. (2002) Desensitization mechanism of GABA receptors revealed by single oocyte binding and receptor function. *J. Neurosci.*, **22**, 7982–7990.
- Chen, C. & Okayama, H. (1987) High-efficiency transformation of mammalian cells by plasmid DNA. *Mol. Cell. Biol.*, **7**, 2745–2752.
- Clements, J.D. (1996) Transmitter timecourse in the synaptic cleft: its role in central synaptic function. *Trends Neurosci.*, **19**, 163–171.
- Colquhoun, D. (1998) Binding, gating, affinity and efficacy: the interpretation of structure-activity relationships for agonists and of the effects of mutating receptors. *Br. J. Pharmacol.*, **125**, 924–947.
- Colquhoun, D. & Sakmann, B. (1985) Fast events in single channel currents activated by acetylcholine and its analogues at the frog muscle end-plate. *J. Physiol.*, **369**, 501–557.
- Colquhoun, D. & Sigworth, F.J. (1995) Fitting and statistical analysis of single-channel records. In Sakmann, B. & Neher, E. (Eds), *Single-Channel Recording*, 2nd Edn. Plenum Press, New York, pp. 231–243.
- Fritschy, J.M. & Brunig, I. (2003) Formation and plasticity of GABAergic synapses: physiological mechanisms and pathophysiological implications. *Pharmacol. Ther.*, **98**, 299–323.
- Gao, B., Fritschy, J.M., Benke, D. & Mohler, H. (1993) Neuron-specific expression of GABA<sub>A</sub>-receptor subtypes: differential association of the alpha 1- and alpha 3-subunits with serotonergic and GABAergic neurons. *Neuroscience*, **54**, 881–892.
- Gingrich, K.J., Roberts, W.A. & Kass, R.S. (1995) Dependence of the GABA<sub>A</sub> receptor gating kinetics on the alpha-subunit isoform: implications for structure-function relations and synaptic transmission. *J. Physiol.*, **489**, 529–543.
- Hutcheon, B., Morley, P. & Poulter, M.O. (2000) Developmental change in GABA<sub>A</sub> receptor desensitization kinetics and its role in synapse function in rat cortical neurons. *J. Physiol.*, **522**, 3–17.
- Jonas, P. (1995) Fast application of agonists to isolated membrane patches. In Sakmann, B. & Neher, E. (Eds), *Single-Channel Recording*, 2nd Edn. Plenum Press, New York, pp. 231–243.
- Jones, M.V. & Westbrook, G.L. (1995) Desensitized states prolong GABA<sub>A</sub> channel responses to brief agonist pulses. *Neuron*, **15**, 181–191.
- Jones, M.V., Sahara, Y., Dzubay, J.A. & Westbrook, G.L. (1998) Defining affinity with the GABA<sub>A</sub> receptor. *J. Neurosci.*, **18**, 8590–8604.
- Lavoie, A.M., Tingey, J.J., Harrison, N.L., Pritchett, D.B. & Twyman, R.E. (1997) Activation and deactivation rates of recombinant GABA<sub>A</sub> receptor channels are dependent on alpha-subunit isoform. *Biophys. J.*, **73**, 2518–2526.
- Macdonald, R.L., Rogers, C.J. & Twyman, R.E. (1989) Kinetic properties of the GABA<sub>A</sub> receptor main conductance state of mouse spinal cord neurones in culture. *J. Physiol.*, **410**, 479–499.
- Maconochie, D.J., Zempel, J.M. & Steinbach, J.H. (1994) How quickly can GABA<sub>A</sub> receptors open? *Neuron*, **12**, 61–71.
- McClellan, A.M. & Twyman, R.E. (1999) Receptor system response kinetics reveal functional subtypes of native murine and recombinant human GABA<sub>A</sub> receptors. *J. Physiol.*, **515**, 711–727.
- Mozrzymas, J.W. (2004) Dynamism of GABA<sub>A</sub> receptor activation shapes the 'personality' of inhibitory synapses. *Neuropharmacology*, **47**, 945–960.
- Mozrzymas, J.W. & Cherubini, E. (1998) Changes in intracellular calcium concentration affect desensitization of GABA<sub>A</sub> receptors in acutely dissociated P2–P6 rat hippocampal neurons. *J. Neurophysiol.*, **79**, 1321–1328.
- Mozrzymas, J.W., Barberis, A., Mercik, K. & Zarnowska, E.D. (2003a) Binding sites, singly bound states, and conformation coupling shape GABA-evoked currents. *J. Neurophysiol.*, **89**, 871–883.
- Mozrzymas, J.W., Zarnowska, E.D., Pytel, M. & Mercik, K. (2003b) Modulation of GABA(A) receptors by hydrogen ions reveals synaptic GABA transient and a crucial role of the desensitization process. *J. Neurosci.*, **23**, 7981–7992.
- Ortinski, P.I., Lu, C., Takagaki, K., Fu, Z. & Vicini, S. (2004) Expression of distinct alpha subunits of GABA<sub>A</sub> receptor regulates inhibitory synaptic strength. *J. Neurophysiol.*, **92**, 1718–1727.

- Overstreet, L.S., Jones, M.V. & Westbrook, G.L. (2000) Slow desensitization regulates the availability of synaptic GABA<sub>A</sub> receptors. *J. Neurosci.*, **20**, 7914–7921.
- Pirker, S., Schwarzer, C., Wieselthaler, A., Sieghart, W. & Sperk, G. (2000) GABA<sub>A</sub> receptors: immunocytochemical distribution of 13 subunits in the adult rat brain. *Neuroscience*, **101**, 815–850.
- Rudolph, U. & Mohler, H. (2004) Analysis of GABA<sub>A</sub> receptor function and dissection of the pharmacology of benzodiazepines and general anesthetics through mouse genetics. *Annu. Rev. Pharmacol. Toxicol.*, **44**, 475–498.
- Rusch, D. & Forman, S.A. (2005) Classic benzodiazepines modulate the open-close equilibrium in alpha1beta2gamma2L gamma-aminobutyric acid type A receptors. *Anesthesiology*, **102**, 783–792.
- Scheller, M. & Forman, S.A. (2002) Coupled and uncoupled gating and desensitization effects by pore domain mutations in GABA<sub>A</sub> receptors. *J. Neurosci.*, **22**, 8411–8421.
- Twyman, R.E., Rogers, C.J. & Macdonald, R.L. (1990) Intraburst kinetic properties of the GABA<sub>A</sub> receptor main conductance state of mouse spinal cord neurones in culture. *J. Physiol.*, **423**, 193–220.
- Verdoorn, T.A. (1994) Formation of heteromeric gamma-aminobutyric acid type A receptors containing two different alpha subunits. *Mol. Pharmacol.*, **45**, 475–480.
- Vicini, S. & Ortinski, P. (2004) Genetic manipulations of GABA<sub>A</sub> receptor in mice make inhibition exciting. *Pharmacol. Ther.*, **103**, 109–120.
- Whiting, P.J. (2003) GABA<sub>A</sub> receptor subtypes in the brain: a paradigm for CNS drug discovery? *Drug Discov. Today*, **8**, 445–450.
- Yee, B.K., Keist, R., von Boehmer, L., Studer, R., Benke, D., Hagenbuch, N., Dong, Y., Malenka, R.C., Fritschy, J.M., Bluethmann, H., Feldon, J., Mohler, H. & Rudolph, U. (2005) A schizophrenia-related sensorimotor deficit links alpha3-containing GABA<sub>A</sub> receptors to a dopamine hyperfunction. *Proc. Natl Acad. Sci. U.S.A.*, **102**, 17 154–17 159.